UNIVERSITY OF CALIFORNIA SAN DIEGO

Associations between baleen whale acoustic occurrence and oceanographic conditions near the South Shetland Islands, Antarctica

A Thesis submitted in partial satisfaction of the requirements
for the degree Master of Science

in

Marine Biology

by

Nicole Schriber

Committee in charge:

Simone Baumann-Pickering, Chair
Kaitlin Frasier
John Hildebrand

2026

The Thesis of Nicole Schriber is approved, and it is acceptable in quality and form for publication on microfilm and electronically.

University of California San Diego

2026

TABLE OF CONTENTS

LIST OF FIGURES

LIST OF TABLES

ACKNOWLEDGEMENTS

First, I would like to thank Dr. Simone Baumann-Pickering for taking a chance on me and giving me this opportunity. I have learned so much over this past year and have gained so many new skills which will help me be a better scientist in the future. Your support means the world to me! I would also like to thank Dr. Natalie Posdaljian for her mentorship. I couldn't have done this without your guidance, and I am so grateful for your kindness and patience.

Thank you as well to Dr. Kaitlin Frasier and Dr. John Hildebrand for agreeing to be part of my committee and taking time out of your busy schedules to do so!

I would also like to thank everyone who has been working on this project for years, making it possible: Trisha Sharan, Sofia Spagarino, Natalie Posdaljian, Jennifer S. Trickey, Ally C. Rice, Megan Wood, Alba Solsona-Berga, Anne Bartlett, Simone Baumann-Pickering, Ana Širović, John A. Hildebrand, M. Vanesa Reyes Reyes, Mariana L. Melćon, Miguel A. Iñíguez, J. Jones, B. Thayre, J. Hurwitz, E. O'Neill, S. Wiggins, Prefectura Naval Argentina, and the officers and crew of the vessel SB-15 Tango. This project also uses data obtained from Archiving, Validation, and Interpretation of Satellite Oceanography (AVISO, https://www.aviso.altimetry.fr/en/home.html), Copernicus Marine Services (https://marine.copernicus.eu/), and General Bathymetric Chart of the Ocean (GEBCO https://www.gebco.net/).

I would also like to thank my family for always supporting me and making it possible for me to achieve this milestone. Thank you especially to my parents, Julia and Mike Schriber. I love you more than anything.

Finally, thank you to all the whales who shaped my journey in life and inspired me to take this path. Every whale leaves an impact, but I would like to send thanks in particular to: Amaya, Nakai, Kalia, Makani, Corky, Orkid, Ulises, Ikaika, Shouka, Keet, Kali, Terso, Diego, Luna, Ewan, Paddy, Marie, Naniyaq, Cloudy, Monti, Theo, and Kulea. You'll never know how much I love you.

Funding was provided by the National Science Foundation, the UCSD Academic Senate, the Consejo Nacional de Investigaciones Científicas y Técnicas, and the Whale and Dolphin Conservation.

This thesis is currently being prepared for publication of the material. Schriber, Nicole; Wood, Megan; Širović, Ana; Posdaljian, Natalie; Hildebrand, John A.; Baumann-Pickering, Simone. The thesis author was the primary investigator and author of this material.

ABSTRACT OF THE THESIS

Associations between baleen whale acoustic occurrence and oceanographic conditions near the South Shetland Islands, Antarctica

by

Nicole Schriber

Master of Science in Marine Biology

University of California San Diego, 2026

Simone Baumann-Pickering, Chair

The Antarctic Peninsula is undergoing rapid environmental change while several baleen whale species continue to recover from historical exploitation. Understanding how whales respond to this dynamic ecosystem is therefore important for identifying the environmental processes that shape feeding habitat. This study examines the acoustic occurrence of humpback (*Megaptera novaeangliae*), fin (*Balaenoptera physalus*), and blue whales (*B. musculus*) near the South Shetland Islands across three site-year deployments between 2014 and 2016. Passive acoustic recordings were used to quantify humpback whale song and non-song vocalizations, fin

whale 20 Hz calls, and blue whale Z- and D-calls. Generalized additive models related acoustic occurrence to environmental variables describing mesoscale circulation, hydrography, primary productivity, and sea ice. Acoustic patterns differed between species, call types, and sites. Fin whale calling showed the clearest seasonality, blue whale Z-calls were persistent year-round, blue whale D-calls occurred in brief episodic events, and humpback whale acoustic occurrence varied strongly among sites. Final models explained 22-69% of deviance, and environmental relationships were predominantly nonlinear. Finite-size Lyapunov exponent (FSLE) magnitude, orientation, or both were retained in 10 of 12 models, making mesoscale structure the most consistently selected environmental component. Chlorophyll *a* was significant in nine models, while temperature, salinity, and dissolved oxygen anomalies, particularly at 130-222 m, were also frequently retained. These results suggest that baleen whale acoustic occurrence near the South Shetland Islands is associated with interacting patterns of mesoscale circulation, water mass variability, productivity, sea ice, and species- or behavior-specific habitat use.

INTRODUCTION

The Southern Ocean was profoundly altered by twentieth-century industrial whaling, when an estimated 2.05 million large whales were killed in the Southern Hemisphere, with blue whales (*Balaenoptera musculus*), fin whales (*B. physalus*), and humpback whales (*Megaptera novaeangliae*) among the most common targets (Rocha et al., 2015). Recovery following protection has been highly uneven. Southern Hemisphere humpback whale stocks have generally increased substantially, although recovery rates differ between populations, and the recent return of large fin whale feeding aggregations to the Antarctic Peninsula has been interpreted as evidence of regional recovery (Herr et al., 2022; Seyboth et al., 2023). Antarctic blue whales, in contrast, remain critically endangered and substantially depleted relative to historical abundance (Branch, 2023; Miller et al., 2024). These changes in whale populations are ecologically important because baleen whales influence marine ecosystems not only through prey consumption, but also through nutrient recycling (Lavery et al., 2014; Nicol et al., 2010). Whale feces contain a high concentration of iron, a limiting nutrient in much of the Southern Ocean, and recent estimates suggest that the larger pre-whaling baleen whale populations recycled considerably more iron and consumed substantially more krill than present-day populations (Lavery et al., 2014; Nicol et al., 2010). Understanding how recovering baleen whales use Southern Ocean habitats is relevant both to their conservation and to understanding the current and future functioning of Antarctic marine ecosystems.

The recovery of these baleen whales is occurring within an environment that is itself changing. The Antarctic Peninsula is among the most rapidly changing regions on Earth due to climate change, with changes in atmospheric and oceanic temperatures, sea ice, and plankton communities having consequences throughout the food web (Clarke et al., 2007; Ducklow et al.,

2007; Krumhardt et al., 2022; Nicol et al., 2008). Ongoing environmental change in the Antarctic Peninsula therefore has the potential to modify baleen whale habitat through changes in the abundance and distribution of their principal prey item: Antarctic krill (*Euphausia superba*).

Antarctic krill provide the primary trophic link between environmental variability and baleen whales in the Southern Ocean. Krill are a major prey resource for humpback, fin, and blue whales, and baleen whale distribution and abundance are frequently associated with krill distribution and availability (Friedlaender et al., 2006; Murase et al., 2002). Krill themselves are strongly influenced by environmental conditions, including sea ice, hydrography, and primary productivity; sea ice influences krill recruitment, habitat, and food availability, while primary production provides food resources for krill (Loeb et al., 2010; Nicol et al., 2008). Consequently, changes in sea ice and productivity may indirectly alter baleen whale habitat by affecting the abundance and distribution of their prey. Relationships between baleen whales and these environmental variables have been observed throughout Antarctic waters; whale distributions have been associated with prey abundance and oceanographic conditions (Friedlaender et al., 2006; Herr et al., 2016), and blue and fin whale acoustic occurrence has been associated with seasonal changes in sea ice concentration (Širović et al., 2004).

These relationships are particularly complex around the South Shetland Islands, where hydrographic conditions and circulation vary over relatively short spatial and temporal scales. This region, located at the northern edge of the Antarctic Peninsula, is an important spawning and nursery habitat for Antarctic krill, but krill recruitment and availability vary significantly among years in association with a hydrographically complex and dynamic environment (Loeb et al., 2010). This region is known for exceedingly complex interactions between water masses and mesoscale structures, which can influence prey habitat over short time scales (García et al., 2002;

Loeb et al., 2010; Patterson & Sievers, 1980; Sangrà et al., 2011; Tokarczyk, 1987). Temperature, salinity, and dissolved oxygen can aid in characterizing these water masses and can therefore provide information about changes in local hydrographic regimes (García et al., 2002), while chlorophyll *a* provides an indicator of phytoplankton biomass and productive conditions. Mesoscale circulation provides an additional source of variability: fronts, filaments, and eddies can bring waters of different origins together and create localized regions of retention or aggregation, which baleen whales have been associated with in other marine systems (Cotte et al., 2011; Fahlbusch et al., 2024). Together, these environmental variables may influence baleen whale habitat, likely through their effects on prey availability and distribution.

Baleen whales are generally considered to be seasonal visitors to Antarctic feeding grounds, migrating to productive high-latitude waters to feed before returning to lower-latitude wintering grounds (Andrews-Goff et al., 2018; Van Opzeeland et al., 2013; Roman et al., 2025). Humpback and fin whales can occur in high numbers during the feeding season, and the region has been identified as important feeding habitat for both species, with blue whales also being known to use feeding grounds in the Antarctic Peninsula (Herr et al., 2016; Johannessen et al., 2022; Trathan et al., 2024). However, seasonal migration does not necessarily result in a complete absence of whales from Antarctic waters during the remainder of the year; acoustic monitoring has documented blue and humpback whale calls during the austral winter (Clarke et al., 2026; Van Opzeeland et al., 2013; Širović et al., 2009). Thus, observations extending beyond the traditional summer survey season are necessary to fully characterize patterns of baleen whale occurrence and their associations with oceanographic conditions.

Studying these patterns in Antarctic waters is challenging, with the remote location, severe weather, and seasonal sea ice restricting ship-based visual surveys for much of the year.

As a result, much of the historical information on Antarctic baleen whale distribution has been collected during the austral summer, when field surveys are most feasible. Passive acoustic monitoring provides an important complement to these observations by allowing recorders to collect data over extended periods and during seasons where visual surveys are difficult or impossible. Long-term acoustic monitoring has improved understanding of the seasonal occurrence and habitat use of baleen whales throughout Antarctic waters (Širović et al., 2004, 2007, 2009; Širović & Hildebrand, 2011; Thomisch et al., 2016). Because these observations measure vocal activity, they provide a record of acoustic occurrence rather than a direct measurement of whale abundance. Nevertheless, they provide temporal coverage that is difficult to achieve through visual surveys alone.

Despite increasing knowledge of baleen whale distribution in Antarctic waters, there remains a need to better understand how whale occurrence relates to environmental variability. Previous studies have established broad seasonal patterns in acoustic occurrence and demonstrated relationships between whales, prey, sea ice, and other environmental conditions (Friedlaender et al., 2006; Herr et al., 2016; Širović et al., 2004; Širović & Hildebrand, 2011). However, the dynamic oceanographic environment surrounding the South Shetland Islands means that local habitat conditions can also vary considerably over relatively short time scales. Integrating long-term acoustic data with concurrent environmental data therefore provides an opportunity to investigate potential associations between environmental variables and baleen whale occurrence.

In this study, we examine the acoustic occurrence of humpback, fin, and blue whales at three sites near the South Shetland Islands between 2014 and 2016. Acoustic detections from Elephant Island, King George Island, and Clarence Island were compared with concurrent

oceanographic variables describing physical conditions, primary productivity, sea ice, and mesoscale circulation. Blue whale Z- and D-calls were considered separately because they represent distinct patterns and behavioral contexts (McDonald et al., 2006; Oleson et al., 2007). Generalized additive models were used to identify nonlinear associations between environmental conditions and baleen whale acoustic occurrence at each site. By comparing multiple species and call types across three locations, this study aims to improve understanding of the environmental conditions associated with baleen whale habitat in the South Shetland Islands and to provide a baseline for evaluating how continued environmental change may affect whale occurrence in the region.

Specifically, we asked (1) how baleen whale acoustic occurrence varied among species, call types, and deployments; (2) which components of the local oceanographic environment were associated with baleen whale acoustic occurrence; and (3) whether the relationships between acoustic occurrence and oceanographic variables were consistent among species, call types, and locations.

METHODS

2.1. STUDY AREA AND PASSIVE ACOUSTIC MONITORING

Passive acoustic monitoring was conducted at three locations in the South Shetland Islands near the northern Antarctic Peninsula: Elephant Island (EI), King George Island (KGI), and Clarence Island (CI) (Figure 1). The Elephant Island recorder was located northwest of the island at 60°53.214′ S, 55°57.238′ W from March 5 to July 17, 2014. The King George Island recorder was located north of the island at 61°27.469′ S, 57°56.515′ W and recorded from February 10, 2015 to January 29, 2016. The Clarence Island recorder was located east of the island at 61°15.112′ S, 53°29.006′ W and recorded from February 4 to December 2, 2016.

The three sites differed in their bathymetry and overall oceanography. The seafloor depth at the King George and Elephant Island sites was approximately 760 m, while the depth at the Clarence Island site was approximately 1,030 m. The Elephant Island site was situated near a comparatively steep bathymetric slope, whereas the King George and Clarence Island sites were adjacent to gentler slopes (Figure 1).

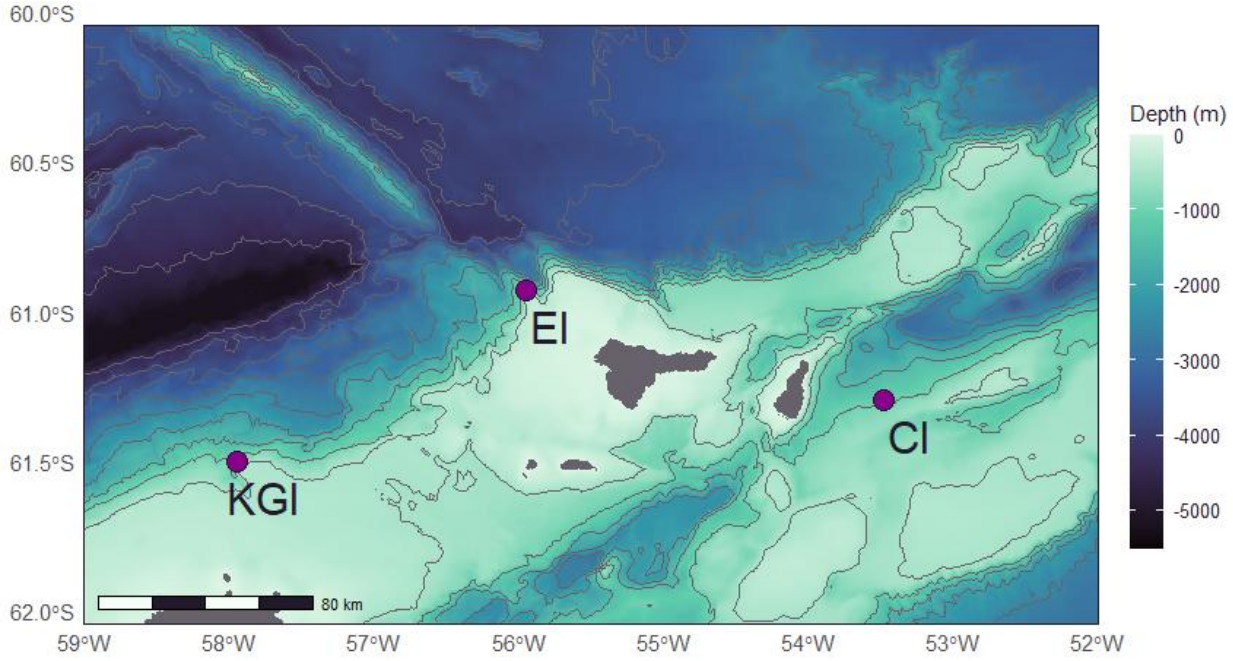

Figure 1. Study area and passive acoustic monitoring locations near the northern Antarctic Peninsula. Purple points indicate High-frequency Acoustic Recording Package (HARP) deployment sites at King George Island (KGI), Elephant Island (EI), and Clarence Island (CI). Background shading and contours indicate seafloor depth (m). Bathymetry data from General Bathymetric Chart of the Ocean (GEBCO; Dorschel et al., 2022). Image credit: Trisha Sharan.

Acoustic data were collected using High-frequency Acoustic Recording Packages (HARPs; Wiggins & Hildebrand, 2007). Each HARP was moored to the seafloor with a hydrophone suspended approximately 10 m above the bottom (Figure 2). All three instruments had a sampling rate of 200 kHz with 16-bit quantization. Hydrophones and systems were appropriately calibrated. Duty cycles differed between sites; the Elephant Island HARP had a duty cycle of 5 minutes of recording followed by 1 minute off, the King George Island HARP had a duty cycle of 10 minutes of recording followed by 3.33 minutes off, and the Clarence Island HARP recorded continuously.

Four baleen whale acoustic response types were analyzed: humpback whale (*Megaptera novaeangliae*) song and non-song vocalizations, fin whale (*Balaenoptera physalus*) 20 Hz calls,

and blue whale (*B. musculus*) Z-calls and D-calls. Blue whale Z- and D-calls were treated separately in the statistical analyses because they were distinct acoustic response variables with substantially different temporal patterns and are known to be behaviorally and ecologically distinct from one another (McDonald et al., 2006; Oleson et al., 2007).

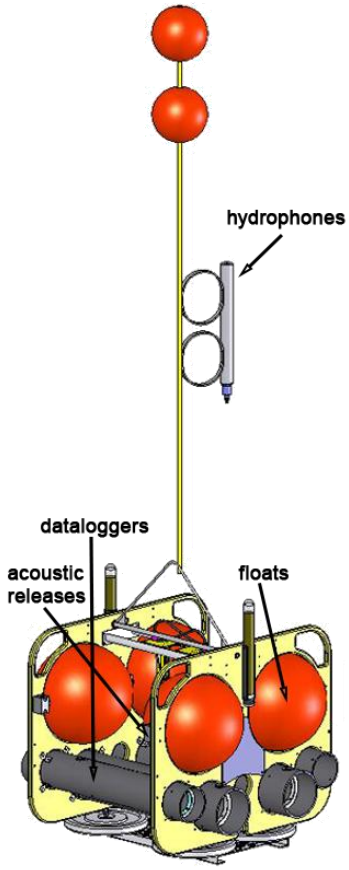

Figure 2. Diagram of the High-frequency Acoustic Recording Package (HARP) used for passive acoustic monitoring. The illustration shows the hydrophone assembly, flotation, acoustic releases, and seafloor-mounted dataloggers. HARP design described by Wiggins and Hildebrand (2007).

2.2. ACOUSTIC DETECTIONS

Species-specific acoustic signals were identified using a combination of manual review in *Triton* (Wiggins et al., 2010), which is a custom acoustic analysis package based in MATLAB

(MathWorks, Natick, MA), and MATLAB-based automated detection algorithms. For humpback whale call analysis, acoustic data were decimated by a factor of 20, producing an acoustic bandwidth of 5 kHz, and for blue and fin whale call analysis, data were decimated by a factor of 100, producing an acoustic bandwidth of 1 kHz. Long-term spectral averages (LTSAs) were calculated using the Welch algorithm (Welch, 1967) with non-overlapping 1 s Hann-windowed frames, yielding 1 Hz frequency resolution, with five consecutive spectra averaged to produce 5 s time bins.

Humpback whale calls (both song and non-song) were detected automatically using a generalized power law (GPL) detector designed to identify the wide variety of humpback whale vocalizations (Helble et al., 2012). Automated detections were subsequently reviewed by a trained analyst, and false detections were removed. The final humpback whale response variable was minutes present per day.

Because fin whale 20 Hz calls frequently overlap, making it difficult to separate individual calls (Širović et al., 2004; Watkins et al., 2000), an energy detector was used to generate a daily acoustic index. The index was calculated as the ratio between the signal near 22 Hz and noise averaged between 10 and 34 Hz (Nieukirk et al., 2012; Širović et al., 2004) power spectral density values from the LTSA (Curtis et al., 1999; Nieukirk et al., 2012; Širović et al., 2004). The resulting daily call index value was used as the fin whale response variable in all analyses.

Blue whale Z-calls were identified by manually scanning 1-h long LTSAs with a time resolution of 5 s and a frequency resolution of 1 Hz. A trained analyst inspected possible calls using a 60-s spectrogram (1500-point fast Fourier transform (FFT) length, 90% overlap).

Presence or absence of Z-calls was recorded for each hour, for a final Z-call response variable of hours present per day.

Blue whale D-calls were detected automatically using a GPL detector that was modified to detect D-calls rather than the humpback whale calls it was originally designed for (Helble et al., 2012). The automated detections were then reviewed by a trained analyst, and false detections were removed. The final D-call response variable was calls per day.

However, there were some gaps in the detector's output due to a timing issue that was observed after analyst verification. Elephant Island had 13 days with unverified gaps, King George Island had 144 days with unverified gaps, and Clarence Island had no days with unverified gaps. The issue was resolved, and the detector was re-run. Rather than manually reviewing each detection again, a verification rate was used to calculate an estimated number of true calls. Manually verified detections were treated as ground truth. For each fully verified day, a verification rate was calculated as the verified detections divided by the total number of detections from the reprocessed detector output. For days containing gaps, a local verification rate was estimated from the nearest fully verified days; neighboring rates were averaged when available, set to zero when both neighboring days contained no verified detections, or replaced with the overall median verification rate when no nearby verified days were available. Reprocessed detections occurring only within the previous gaps were then multiplied by the estimated verification rate. This approach preserved the original manually verified dataset while conservatively estimating detections missed because of the detector timing issue.

2.3. ENVIRONMENTAL DATA

The oceanographic variables used in the final baleen whale modeling dataset included measurements representing mesoscale circulation, primary productivity, water mass properties, and sea ice conditions. Environmental data, from both satellite-derived and modeled datasets, were extracted for a region extending 40 x 40 km around each recording site at a daily resolution. Environmental variables retained in the modeling dataset were obtained from AVISO+ (Archiving, Validation, and Interpretation of Satellite Oceanography) and Copernicus Marine (AVISO+, 2018; E.U. Copernicus Marine Service Information, 2023, 2024).

Mesoscale activity was characterized using backward-in-time finite-size Lyapunov exponents (FSLE). Backward-in-time FSLE fields identify regions of convergence and can delineate fronts, filaments, and eddy boundaries (d'Ovidio et al., 2004, 2010). Daily, 0.04° backward-in-time FSLE fields were obtained from the delayed-time global all-satellite FSLE product distributed by AVISO+ (AVISO+, 2018). FSLE magnitude was used to represent the strength of convergence zones. More negative values represented higher convergence strength.

FSLE fields were also used to characterize the spatial orientation of mesoscale structures. Because FSLE ridges can delineate a variety of oceanographic features, including sharp fronts, narrow filaments, and mesoscale eddy boundaries, the neutral term ridge orientation is used here to describe their spatial alignment. Ridge orientation represents the local orientation of an FSLE ridge and is defined by the angle perpendicular to the local FSLE gradient vector (Bloom et al., 2025). In the source data, orientation was measured anticlockwise relative to east. For analysis, the resulting orientation values were expressed in degrees relative to the north-south axis, with 0° representing a north-south alignment and ± 90° representing an east-west alignment.

Temperature, salinity, and sea ice concentration were obtained from the Copernicus Marine GLOBAL_MULTIYEAR_PHY_001_030 Global Ocean Physics Reanalysis (E.U. Copernicus Marine Service Information, 2023), which had a spatial resolution of 0.083° and a daily temporal resolution. Dissolved oxygen and chlorophyll *a* were obtained from Copernicus Marine GLOBAL_MULTIYEAR_BGC_001_029 Global Ocean Biogeochemistry Hindcast (E.U. Copernicus Marine Service Information, 2024), which had a spatial resolution of 0.25° and a daily temporal resolution.

Once environmental variables were obtained, the daily values were spatially averaged across all model grid cells within the extraction region surrounding each recording site. Variables were averaged separately at each available depth. Because data availability differed among variables and depths, only the depths at which all variables existed were retained. Variables for which data at multiple depths existed were then averaged over two depth bins: 0-54 m and 130-222 m, explained in more detail in section 2.3.2.

2.3.1. Deseasoning procedure

For certain variables that displayed a clear seasonal trend, anomalies were used in place of the raw data. To isolate anomalous variability from the underlying seasonal cycle, environmental predictors were converted to anomalies relative to a site-specific climatological baseline constructed from a 10-year historical time series. The variables retained in the final models that were subjected to this deseasoning procedure were temperature, salinity, and oxygen. The deseasoning procedure was done using the software *R* using the *stats* package (R Core Team, 2025). For each site and variable, a monthly climatology was first calculated by averaging all observations within each calendar month across the full 10-year historical period.

To avoid discontinuities associated with treating the monthly climatology as a series of discrete monthly means, the 12 monthly averages were fitted with a periodic cubic smoothing spline (stats::splinefun, method = "periodic"). Each monthly mean was anchored to the 15th day of the corresponding month using a non-leap-year day-of-year reference grid. The periodic boundary condition constrained the fitted seasonal cycle to transition smoothly between December and January, producing a continuous seasonal baseline throughout the year. For each observation, the fitted climatological value was evaluated at the corresponding day of the year, and the anomaly was calculated as the observed value minus that day's seasonal baseline. This procedure was performed independently for each site and variable and was applied consistently to both the native daily data and the autocorrelation-informed temporally binned data used for model fitting. Environmental anomalies retained their original units and were not standardized to unit variance prior to model fitting.

2.3.2. Depth binning

Variables with data across depths (temperature, salinity, oxygen, and chlorophyll *a*) were averaged into two depth bins for baleen whale analysis: 0-54 m and 130-222 m. The decision on where to divide the depth bins was based on the depths at which temperature, salinity, and oxygen changed rapidly, with the aim of sampling a representative section of both shallow and deep waters (Figure 3). The exact depths at which these bins began and ended were based on which depths had available data. Spatial averaging occurred first at each depth before binning, and then matched depths were grouped into the two depth bins using an unweighted arithmetic mean. The deeper bin was included to characterize variability in the subsurface water that would not be apparent from surface conditions and is known to be relevant foraging habitat for these

baleen whale species (Croll et al., 2001; Ware et al., 2011). Temperature was retained as a candidate variable in both the 0-54 m and 130-222 m bins, chlorophyll *a* in only the 0-54 m bin, and salinity and oxygen in only the 130-222 m bin. The decision to exclude the shallower depths for salinity and oxygen and the deeper depth for chlorophyll was made after several iterations of preliminary models, where they were rarely retained. This will be further explained in section 2.4.2.

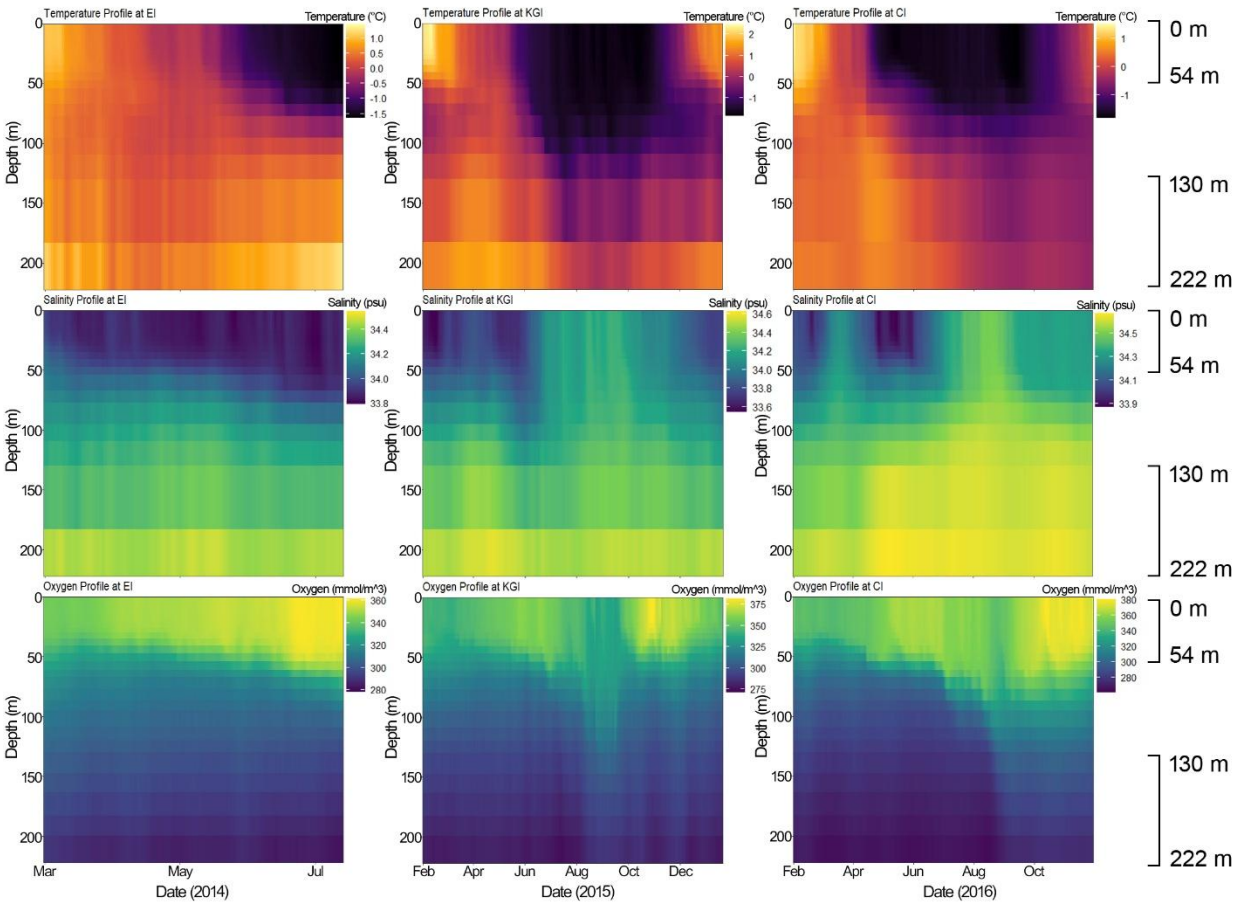

Figure 3. Vertical structure of temperature, salinity, and dissolved oxygen used to inform selection of depth bins. Time-varying vertical profiles are shown for Elephant Island (EI; left), King George Island (KGI; middle), and Clarence Island (CI; right), with temperature, salinity, and dissolved oxygen shown from top to bottom. Color gradients illustrate changes in each environmental variable throughout the water column and over the recording period. Brackets at the right indicate the two depth ranges used to construct environmental predictors for subsequent analysis: 0-54 m and 130-222 m. These intervals were selected to represent distinct shallow and subsurface portions of the water column separated by a region of pronounced vertical change in hydrographic conditions.

2.4. MODELING

Generalized Additive Models (GAMs; Hastie & Tibshirani, 1990) were used as a modeling framework and performed in the software R version 4.5.1 (R Core Team, 2025) to test the significance of environmental predictors on baleen whale call types at each site.

2.4.1. Autocorrelation

Initial environmental and acoustic data were organized at a daily resolution. Because observations on consecutive days were temporally autocorrelated, autocorrelation was evaluated separately for each site before fitting the final GAMs. Initially, for each site and acoustic response type, a preliminary Tweedie GAM was fitted to the daily response using a set of representative environmental predictors with the *mgcv* package in *R* (Wood, 2011; R Core Team, 2025). The Tweedie family was selected because all four response variables were nonnegative, included zero values, and displayed continuous or highly overdispersed positive distributions after temporal aggregation. The use of a common family also allowed for a consistent modeling framework across acoustic response types. Smooth terms used a maximum basis dimension of $k = 4$ with the smoothing parameter fixed at $sp = 0.1$, and the preliminary models were fitted using restricted maximum likelihood (REML). Residual autocorrelation functions (ACFs) were then calculated using the function *acf()* in the *R* package *stats* (R Core Team, 2025), with ACF confidence intervals obtained using the *ggfortify* package (Tang et al., 2016). The first lag at which the residual autocorrelation fell below the upper 95% confidence limit was used as an initial estimate of the temporal bin width. This procedure was used to produce an initial temporal bin size for each site and acoustic response type. Because the resulting ACF-based estimates were generally similar within sites, differing by approximately 1-2 days, a common bin width was selected for each site to allow for direct comparison among results within each site. Final bin widths were 3 days at Elephant Island, 4 days at King George Island, and 4 days at Clarence Island. Daily acoustic and environmental observations within each bin were averaged to produce the dataset used in subsequent modeling.

2.4.2. Pre-selection process

Collinearity among candidate predictors was evaluated using the function *vif (*variance inflation factor) calculated with the *car* package in *R* (Fox & Weisberg, 2019). Screening was conducted separately for each site. Beginning with all available candidate predictors, the variable with the largest VIF was sequentially removed until all remaining variables had a VIF ≤ 5.

Because temperature anomaly was kept as a candidate variable at both depth bins, one depth was removed to prevent multiple representations of temperature from entering the model. For each model, the two competing candidate variables, temperature anomaly at 0-54 m and temperature anomaly at 130-222 m, were compared using separate univariate GAMs built using the function *gam* in the *mgcv* library in *R* (Wood, 2011; R Core Team, 2025). Each model contained a single smooth term with a maximum basis dimension of $k = 4$, was modeled using a Tweedie error distribution with a log link, and was fitted using restricted maximum likelihood (REML). The final modeling code specified the Tweedie family as 'tw(link = "log", a = 1.1, b = 1.9).' The two candidate temperature variables were ranked by Akaike's Information Criterion (AIC; Akaike, 1974), calculated with the *AIC()* function in the *R* package *stats* (R Core Team, 2025), and the variable producing the lower AIC value was selected to continue through the modeling process.

Initially, salinity anomaly at 0-54 m, oxygen anomaly at 0-54 m, and chlorophyll *a* at 130-222 m were included as candidate variables and evaluated using the same process described above for temperature. However, these variables at these depth bins were consistently removed during the pre-selection process and rarely made it through to the final models. The differences in AIC values between competing depth bins for these variables were minimal, so the decision was made to remove these less relevant bins. In the case of temperature, both bins were chosen

often enough, and AIC values were not always similar enough, to justify removing one depth from the list of candidate variables.

2.4.3. Generalized Additive Models

Separate GAMs were developed for each combination of recording site and acoustic response type, producing 12 final models. Acoustic response variables were modeled as described in the previous section. Smooth terms were fitted independently for each environmental predictor, and additional smooth-term penalization was enabled using 'select = TRUE.'

An initial model was constructed using FSLE magnitude, FSLE orientation, salinity anomaly at 130-222 m, dissolved oxygen anomaly at 130-222 m, chlorophyll *a* concentration at 0-54 m, sea ice concentration, and the predictor selected for temperature anomaly. Backward selection was then performed on the basis of approximate significance tests for the GAM smooth terms obtained with the *summary.gam()* method in the *mgcv* package (Wood, 2011, 2013). At each iteration, the predictor with the largest smooth-term p-value was removed, and the model was refitted. This process was repeated until all remaining smooth terms had $p \leq 0.05$.

Final GAMs were evaluated using residual diagnostic plots and model checks implemented in the *mgcv* and *gratia* packages (Simpson, 2024; Wood, 2011, 2013). Simulated quantile-quantile plots, residual histograms, residuals plotted against the linear predictor, and observed-versus-fitted values were examined for evidence of departures from the assumed Tweedie response distribution or systematic residual patterns. The adequacy of smooth-term basis dimensions was assessed using 'gam.check(),' with low k-index values and associated p-values used to identify potentially inadequate basis dimensions. Deviance residuals were also

plotted through time and residual autocorrelation functions were examined to assess whether temporal structure remained following autocorrelation-informed temporal binning.

RESULTS

3.1. PATTERNS IN ACOUSTIC OCCURRENCE

All four acoustic response types were detected at each site but differed temporally between call type and site (Figure 4). Because acoustic occurrence was measured differently between species, absolute magnitudes of the acoustic response variables are not directly comparable. Comparisons are therefore based on temporal patterns and relative changes in magnitude. Broadly, blue whale Z-calls were the most persistent and consistent (Figure 4c), while, in contrast, blue whale D-calls were concentrated into comparatively brief calling events (Figure 4d). Fin whales showed persistence throughout the monitored periods with distinct peaks in occurrence (Figure 4b), and humpback whales showed higher variability in acoustic occurrence between sites (Figure 4a).

Figure 4. Daily baleen whale acoustic occurrence across three recording sites.

Acoustic response variables are shown for (a) humpback whales, expressed as minutes per day, (b) fin whales, expressed as the daily 20 Hz call index, (c) blue whale Z-calls, expressed as hours present per day, and (d) blue whale D-calls, expressed as calls per day. Each panel shows Elephant Island, King George Island, and Clarence Island. Gray shading denotes periods without acoustic recording effort. Because acoustic occurrence was quantified differently among response types, magnitudes should not be compared directly between panels.

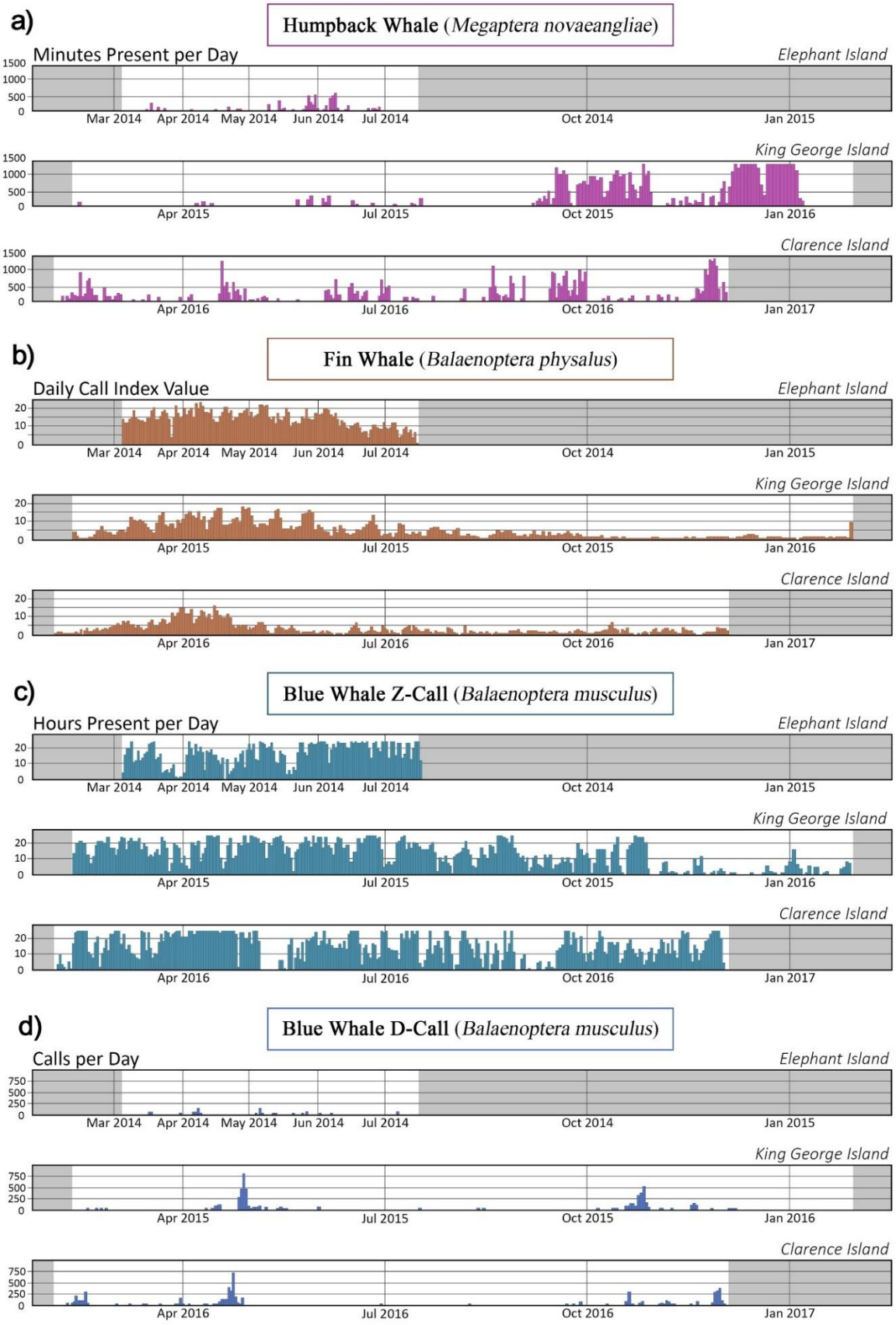
a)
Humpback Whale (Megaptera novaeangliae)
Minutes Present per Day
Elephant Island
King George Island
Clarence Island
b)
Fin Whale (Balaenoptera physalus)
Daily Call Index Value
c)
Blue Whale Z-Call (Balaenoptera musculus)
Hours Present per Day
d)
Blue Whale D-Call (Balaenoptera musculus)
Calls per Day
Mar 2014
Apr 2014
May 2014
Jun 2014
Jul 2014
Oct 2014
Jan 2015
Apr 2015
Jul 2015
Oct 2015
Jan 2016
Apr 2016
Jul 2016
Oct 2016
Jan 2017

3.1.1. Elephant Island

Recording at Elephant Island extended from March 2014 to July 2014. Humpback whale acoustic occurrence was substantially lower and more intermittent than at King George or Clarence Islands. Detections were scattered throughout the recording period, with the largest peak in occurrence occurring between mid-May and mid-June. Even during this period of peak occurrence, a maximum of approximately 500 minutes of acoustic presence were recorded per day (Figure 4a).

In contrast, fin whale calling was persistent at Elephant Island, being detected every day of the recording period. Calling was strongest from March through mid-June, when daily call index values frequently exceeded 15. Calling then began to decrease gradually toward the end of the deployment period, though index values still often reached 10 (Figure 4b).

Similarly, blue whale Z-calls were present consistently throughout the deployment, though they showed more fluctuation in magnitude. Z-calls were often present for 15-24 hours per day during most of the recording period, but three distinct decreases in calling occurred in late March, mid-April, and mid-May. Each decline was followed by renewed high levels of daily occurrence that did not indicate a seasonal trend (Figure 4c).

As at other sites, blue whale D-calls were highly sporadic, though maximum daily counts were lower than at King George and Clarence Islands. Most days contained few or no calls, with isolated calling events occurring during mid-March, April, May, June, and July (Figure 4d).

Elephant Island showed sustained fin whale and Z-call occurrence throughout the entire deployment, accompanied by only occasional humpback whale and D-call activity (Figures 4a-d). The short deployment period makes it difficult to evaluate any seasonal trends.

3.1.2. King George Island

Recording at King George Island lasted for approximately one year, beginning in February 2015 and ending in late January 2016. Humpback whale acoustic occurrence was low and sporadic from March through August. Occurrence increased rapidly during the month of September and remained elevated through much of October, decreasing in November before increasing once again from December through mid-January, after which calling ceased (Figure 4a).

Fin whale 20 Hz calls were recorded throughout the year. Call index values were relatively high and persistent from approximately March through June. Acoustic occurrence declined through July and August and remained comparatively low from September through January (Figure 4b).

Blue whale Z-calls were detected on most recording days from mid-February, when recording began, through October, often reaching 20-24 hours of acoustic occurrence. Daily occurrence became more variable and began to decline in November. The remainder of the year showed more sporadic detections (Figure 4c).

Blue whale D-calls were detected much less continuously than Z-calls and occurred in two distinct episodes. The first calling event occurred near the beginning of May, when calls increased sharply, reaching a maximum of nearly 800 calls per day. The second major calling period occurred in late October, when a maximum of approximately 500 calls per day was reached (Figure 4d).

Overall, King George Island was characterized by relatively persistent fin whale and Z-call occurrence during the first half of the deployment period, followed by a substantial increase

in humpback whale acoustic occurrence during spring and early summer (Figures 4a-d). D-call activity overlapped with both periods but was restricted to relatively short pulses.

3.1.3. Clarence Island

Recording at Clarence Island began in early February 2016 and ended around the beginning of December 2016. Humpback whale acoustic occurrence was highly episodic, with distinct periods of elevated acoustic occurrence in mid-February, late April, June, late August, late September, and late November (Figure 4a). The period with the maximum number of detections per day was in late November, when humpback whale acoustic occurrence exceeded 1,000 minutes per day for multiple days (Figure 4a).

As at the other sites, fin whales were detected throughout the deployment period, though there was a substantial increase in acoustic activity from mid-February through mid-May (Figure 4b). Clarence Island showed the most distinct seasonal trend for fin whales, with activity peaking in April with a gradual increase and decrease on either end of the event (Figure 4b). Low-level calls then persisted throughout the deployment (Figure 4b).

Z-calls were detected on most days throughout the deployment, with calling activity peaking in April when most days recorded over 20 hours of acoustic occurrence per day (Figure 4c). A brief, sharp drop in activity occurred near the beginning of May (Figure 4c). Calling then resumed in mid-May and lasted through the end of August before another decline occurred (Figure 4c). This was followed by another increase in activity that lasted through the end of the deployment (Figure 4c).

D-calls showed the same episodic trend as at other sites, with low acoustic occurrence throughout the deployment period punctuated by discrete calling events (Figure 4d). The largest

of these events occurred in mid-February, late April, mid-October, and late November (Figure 4d). The late April event was the most substantial, when counts approached 700 calls per day (Figure 4d). Calling events at Clarence Island are comparable in magnitude to those at King George Island (Figure 4d).

Clarence Island was overall dominated by persistent blue whale Z-calls, with a seasonal peak in fin whale acoustic occurrence, and episodic calling events for both humpback whales and blue whale D-calls (Figures 4a-d).

3.2. SITE-SPECIFIC OCEANOGRAPHY

Oceanographic conditions varied over time and among the three recording sites (Figures 5 through 7). In particular, the fluctuations in temperature, salinity, and dissolved oxygen anomalies varied substantially between sites. These anomalies showed more short-term variability at Elephant and King George Islands than at Clarence Island (Figures 5 through 7). However, there were also consistencies among the sites, particularly with variables that captured a seasonal trend (Figures 5 through 7). Seasonal patterns were especially apparent in chlorophyll *a* and sea ice concentration at King George and Clarence Islands, the two sites with deployments long enough to capture seasonal trends (Figures 6 and 7). Chlorophyll *a* concentration exhibited a small peak in autumn and a sharp increase during spring (Figures 6 and 7). Sea ice at these sites increased through the winter and subsequently declined during spring (Figures 6 and 7).

The shorter Elephant Island deployment captured a similar autumn peak in chlorophyll *a* concentration and an increase in sea ice concentration near the end of the deployment period (Figure 5). However, because Elephant Island was sampled for only approximately four months, these patterns cannot be interpreted as representative of its complete annual cycle. As a result,

during the deployment time, sea ice concentration at Elephant Island was low and a maximum chlorophyll *a* concentration was reached in autumn, rather than spring (Figures 5 through 7).

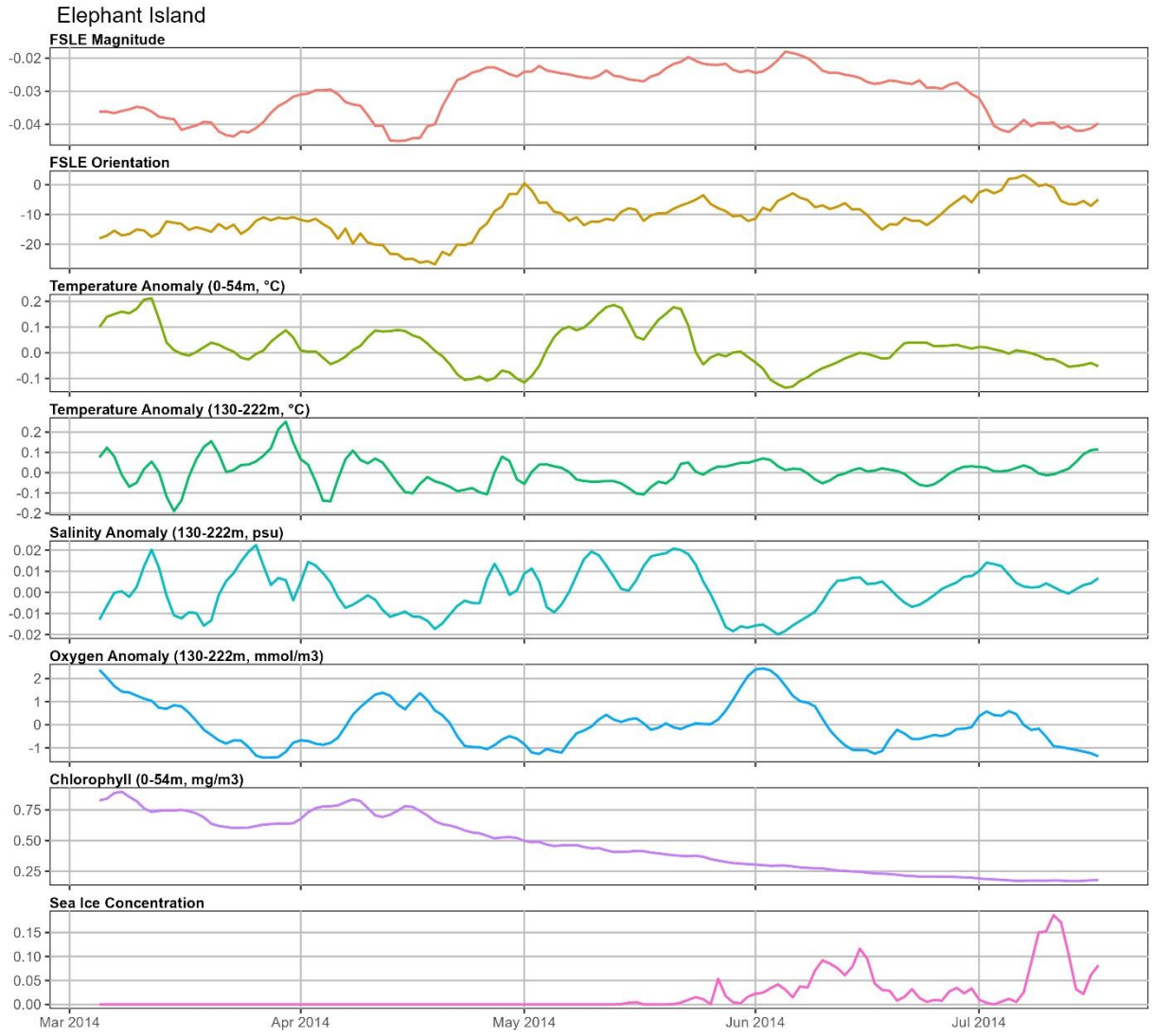

Figure 5. Environmental time series at Elephant Island during the March-July 2014 deployment. Variables displayed, from top to bottom, are backward-in-time finite-size Lyapunov exponent (FSLE) magnitude, FSLE orientation, temperature anomaly at 0-54 m, temperature anomaly at 130-222 m, salinity anomaly at 130-222 m, dissolved oxygen anomaly at 130-222 m, chlorophyll a concentration at 0-54 m, and sea ice concentration. Temperature, salinity, and oxygen are shown as anomalies relative to site-specific seasonal climatologies, with positive and negative values representing conditions above and below the expected seasonal baseline. Chlorophyll a and sea ice concentration are shown as raw values. Because the Elephant Island deployment covered only approximately four months, the time series represents only a partial seasonal record.

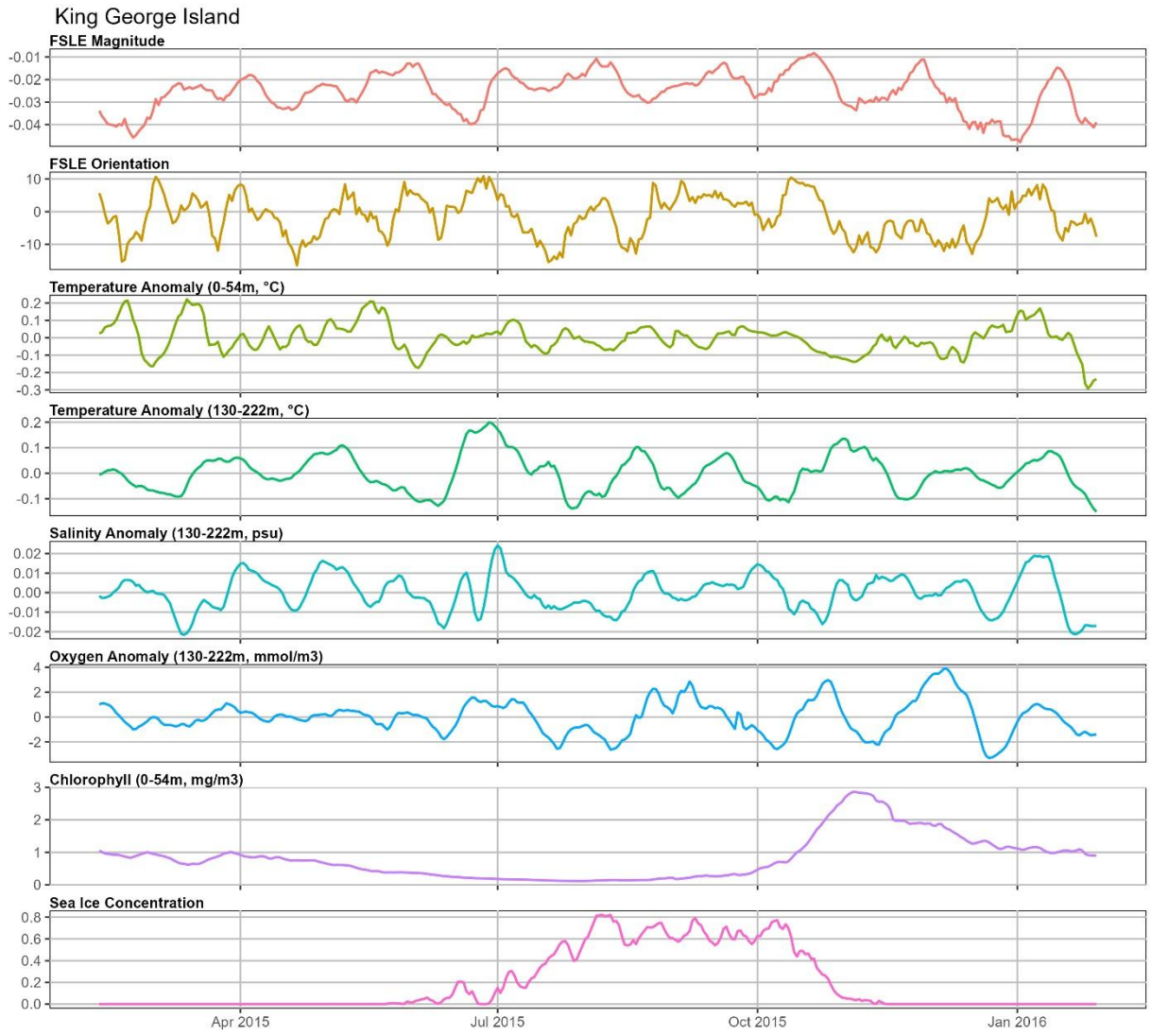

Figure 6. Environmental time series at King George Island during the February 2015-January 2016 deployment. Variables displayed, from top to bottom, are backward-in-time finite-size Lyapunov exponent (FSLE) magnitude, FSLE orientation, temperature anomaly at 0-54 m, temperature anomaly at 130-222 m, salinity anomaly at 130-222 m, dissolved oxygen anomaly at 130-222 m, chlorophyll a concentration at 0-54 m, and sea ice concentration. Temperature, salinity, and oxygen are shown as anomalies relative to site-specific seasonal climatologies, with positive and negative values representing conditions above and below the expected seasonal baseline. Chlorophyll a and sea ice concentration are shown as raw values.

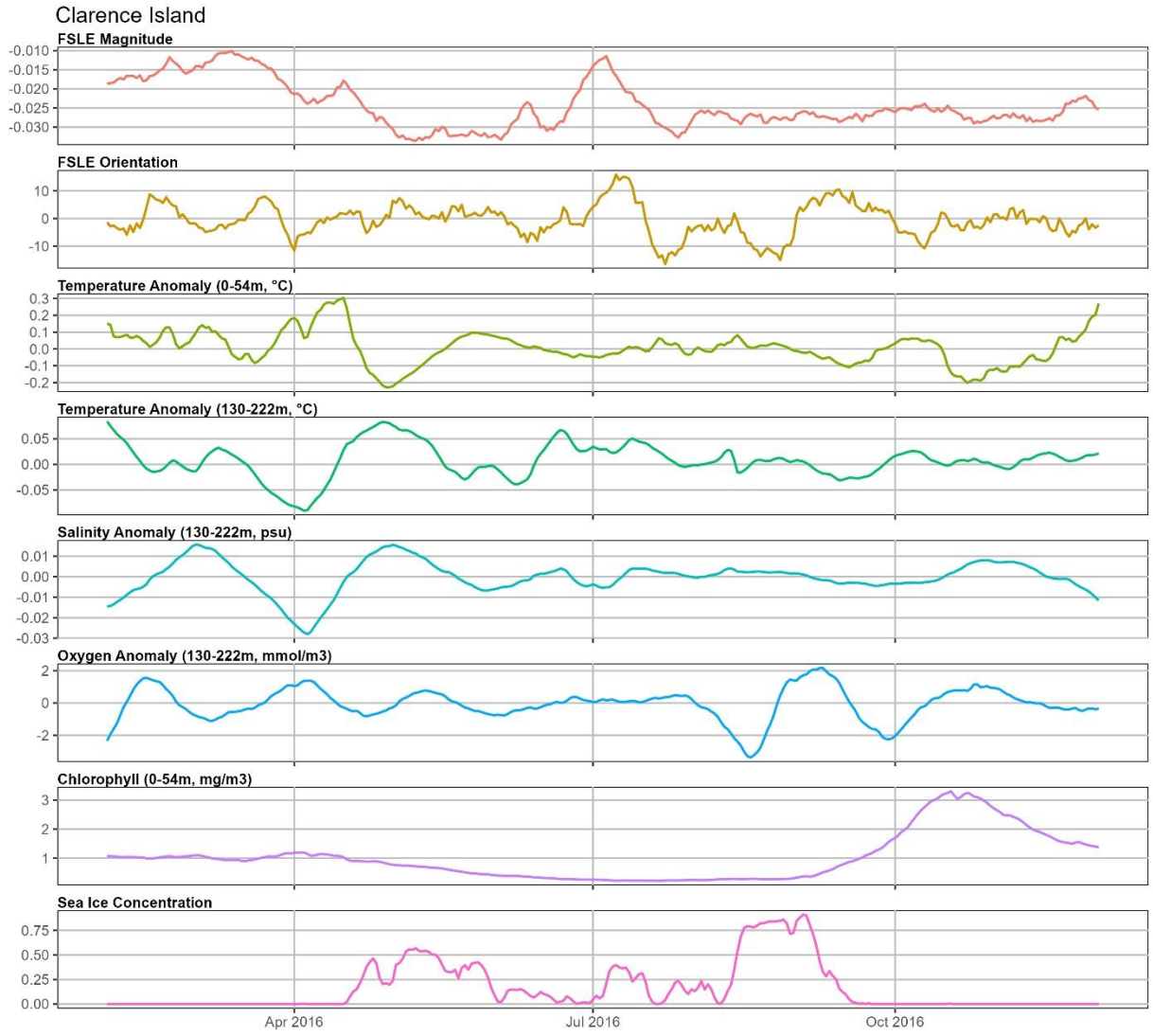

Figure 7. Environmental time series at Clarence Island during the February-December 2016 deployment. Variables displayed, from top to bottom, are backward-in-time finite-size Lyapunov exponent (FSLE) magnitude, FSLE orientation, temperature anomaly at 0-54 m, temperature anomaly at 130-222 m, salinity anomaly at 130-222 m, dissolved oxygen anomaly at 130-222 m, chlorophyll a concentration at 0-54 m, and sea ice concentration. Temperature, salinity, and oxygen are shown as anomalies relative to site-specific seasonal climatologies, with positive and negative values representing conditions above and below the expected seasonal baseline. Chlorophyll a and sea ice concentration are shown as raw values.

3.3. MODELS

A generalized additive model (GAM) was produced for each call type at each site, resulting in twelve total models that examined the relationships between whale acoustic occurrence and oceanographic conditions. Model performance varied among species, call types, and sites, with deviance explained ranging from 22% to 69% (Table 1). Four of the twelve models explained more than 50% of the deviance (Table 1). Mesoscale variables, represented by FSLE, were the most consistently retained predictors, with FSLE magnitude, FSLE orientation, or both being significant in ten out of the twelve models (Table 1). Chlorophyll was also frequently selected, being significant in nine out of the twelve models (Table 1). Deseasoned temperature, salinity, and oxygen variables were often significant, but were selected less consistently across species and sites; temperature anomaly was significant in six models, salinity anomaly in four, and oxygen anomaly in five (Table 1). Sea ice concentration was significant in four models (Table 1). Responses to the environmental predictors were predominantly nonlinear (Figures 8, 10, and 12). Most smooths displayed peaks at intermediate values, plateaus, or U-shaped relationships (Figures 8, 10, and 12). Consequently, acoustic occurrence was rarely associated with a uniform increase or decrease in environmental variables.

Table 1. Summary of final generalized additive models (GAMs) relating baleen whale acoustic occurrence to environmental predictors at Elephant Island (EI), King George Island (KGI), and Clarence Island (CI).

Separate models were fitted for humpback whale calls, fin whale 20 Hz calls, blue whale Z-calls, and blue whale D-calls. Bin size indicates the autocorrelation-informed temporal bin width in days, and *n* represents the number of temporally binned observations used in each model. Model fit is summarized by the percent deviance explained and adjusted R^2. Only environmental predictors retained in the final models are shown. For each retained predictor, the effective degrees of freedom (edf), F-statistic, and approximate smooth-term p-value are reported. Asterisks indicate statistical significance ($p \leq 0.05$*, $p \leq 0.01$**, $p \leq 0.001$***).

Site	Response variable	Bin size (d)	n	Deviance explained (%)	R^2 adjusted	Predictor variable edf F-statistic p-value				
						FSLE magnitude	FSLE orientation	Oxygen anomaly (130-222 m)	Salinity anomaly (130-222 m)	
						1.57	1.61	1.48	0.86	
	Humpback					3.52	2.04	1.74	1.99	
EI	whale calls	3	47	61.0	0.53	0.002**	0.025*	0.033*	0.008**	
						FSLE magnitude	Chlorophyll *a*	Oxygen anomaly (130-222 m)		
						0.90	1.98	0.91		
	Fin whale 20					3.02	20.33	3.03		
EI	Hz calls	3	47	65.0	0.66	0.002**	<0.001***	0.002**		
						Chlorophyll *a*	Salinity anomaly (130-222 m)	Temperature anomaly (130-222 m)		
						1.75	0.77	1.84		
	Blue whale Z					6.13	1.08	2.30		
EI	calls	3	47	49.0	0.49	<0.001***	0.045*	0.02*		
						FSLE orientation	Chlorophyll *a*			
						1.39	0.95			
	Blue whale D					5.57	6.49			
EI	calls	3	47	22.2	-0.09	<0.001***	<0.001***			
						FSLE magnitude	Chlorophyll *a*	Ice concentration		
						1.78	1.89	1.76		
	Humpback					4.55	12.84	10.01		
KGI	whale calls	4	93	46.8	0.46	<0.001***	<0.001***	<0.001***		
						FSLE magnitude	Chlorophyll *a*	Temperature anomaly (0-54 m)	Ice concentration	
						2.05	1.96	1.45	1.88	
	Fin whale 20					7.29	51.67	2.65	21.95	
KGI	Hz calls	4	93	69.0	0.56	<0.001***	<0.001***	0.005**	<0.001***	
						Chlorophyll *a*	Oxygen anomaly (130-222 m)			
						1.83	1.64			
	Blue whale Z					9.53	3.03			
KGI	calls	4	93	31.5	0.35	<0.001***	0.006**			
						FSLE magnitude	FSLE orientation	Chlorophyll *a*	Temperature anomaly (130-222 m)	
						0.95	1.68	2.32	0.91	
	Blue whale D					6.89	5.76	11.79	3.24	
KGI	calls	4	93	41.2	0.03	<0.001***	<0.001***	<0.001***	0.001**	
						FSLE magnitude	Chlorophyll *a*	Salinity anomaly (130-222 m)	Temperature anomaly (0-54 m)	Ice concentration
						1.85	1.85	1.99	0.81	1.57
	Humpback					5.77	6.60	3.37	1.33	1.73
CI	whale calls	4	81	38.6	0.40	<0.001***	<0.001***	0.005**	0.03*	0.04*
						FSLE magnitude	Oxygen anomaly (130-222 m)	Salinity anomaly (130-222 m)		
						1.58	1.78	1.89		
	Fin whale 20					4.08	4.58	8.71		
CI	Hz calls	4	81	48.4	0.47	<0.001***	<0.001***	<0.001***		
						FSLE magnitude	Oxygen anomaly (130-222 m)	Temperature anomaly (130-222 m)		
						1.63	1.89	0.96		
	Blue whale Z					2.77	8.61	2.10		
CI	calls	4	81	33.1	0.29	0.009**	<0.001***	0.009**		
						FSLE magnitude	Chlorophyll *a*	Temperature anomaly (130-222 m)	Ice concentration	
						2.16	2.56	0.86	1.69	
	Blue whale D					9.49	10.91	2.02	2.35	
CI	calls	4	80	57.7	0.24	<0.001***	<0.001***	0.009**	0.02*	

3.3.1. Elephant Island

The humpback whale model explained 61% of the deviance at Elephant Island (Table 1). Humpback whale acoustic occurrence was significantly associated with FSLE magnitude ($p = 0.002$), FSLE orientation ($p = 0.025$), oxygen anomaly between 130-222 m ($p = 0.033$), and salinity anomaly between 130-222 m ($p = 0.008$; Table 1). Occurrence generally increased as FSLE values became less negative, with a dip towards more negative values (Figures 8 and 9). However, there was greater uncertainty at the lower end of the observed range (Figure 8). FSLE orientation had a broad intermediate optimum, though uncertainties were greater at both ends of the observed range (Figures 8 and 9). Deep oxygen anomaly also showed an intermediate optimum, at a moderately positive anomaly, with a similar increase in uncertainty towards both ends of the range (Figure 8). Acoustic occurrence showed a negative relationship with salinity anomaly (Figure 8).

The fin whale 20 Hz model explained 65% of the deviance at Elephant Island (Table 1). Occurrence was significantly associated with FSLE magnitude ($p = 0.002$), chlorophyll *a* ($p < 0.001$), and oxygen anomaly between 130-222 m ($p = 0.002$; Table 1). Occurrence increased nearly linearly as FSLE values and oxygen anomaly became less negative (Figures 8 and 9). Chlorophyll *a* showed a narrow optimum at moderately high values, with occurrence increasing rapidly at lower values (Figure 8).

The blue whale Z-call model explained 49% of the deviance at Elephant Island (Table 1). Z-call occurrence was significantly associated with chlorophyll *a* ($p < 0.001$), salinity anomaly between 130-222 m ($p = 0.045$), and temperature anomaly between 130-222 m ($p = 0.02$; Table 1). Acoustic occurrence had a U-shaped relationship with chlorophyll *a*, with greater occurrence at low and high concentrations (Figure 8). Z-call occurrence declined as the 130-222 m salinity

anomaly became more positive (Figure 8). Occurrence was relatively stable across cooler and near-average deep temperature anomalies but declined under the warmest anomalies (Figure 8).

The blue whale D-call model explained 22% of the deviance at Elephant Island (Table 1). D-call occurrence was significantly associated with FSLE orientation ($p < 0.001$) and chlorophyll *a* ($p < 0.001$; Table 1). Occurrence increased as FSLE orientation values became less negative (Figures 8 and 9). A positive relationship was also seen with chlorophyll *a* concentration (Figure 8).

Figure 8. Estimated partial effects of environmental predictors retained in final generalized additive models (GAMs) for baleen whale acoustic occurrence at Elephant Island.

Rows represent, from top to bottom, humpback whale calls, fin whale 20 Hz calls, blue whale Z-calls, and blue whale D-calls. Columns represent the environmental predictors considered during the modeling process. Black curves show the estimated partial effect of each retained predictor, shaded bands indicate 95% confidence intervals, and the rug marks along the x-axis indicate the distribution of observed predictor values. Asterisks indicate smooth-term significance ($p \leq 0.05$*, $p \leq 0.01$**, $p \leq 0.001$***). Gray cells indicate predictors excluded during the pre-selection process, whereas empty white cells indicate predictors that passed pre-selection but were not retained in the final model. Predictor x-axis limits are held constant for each variable across Figures 8, 10, and 12 and span the combined range across sites to facilitate comparison. Y-axis limits vary between smooths.

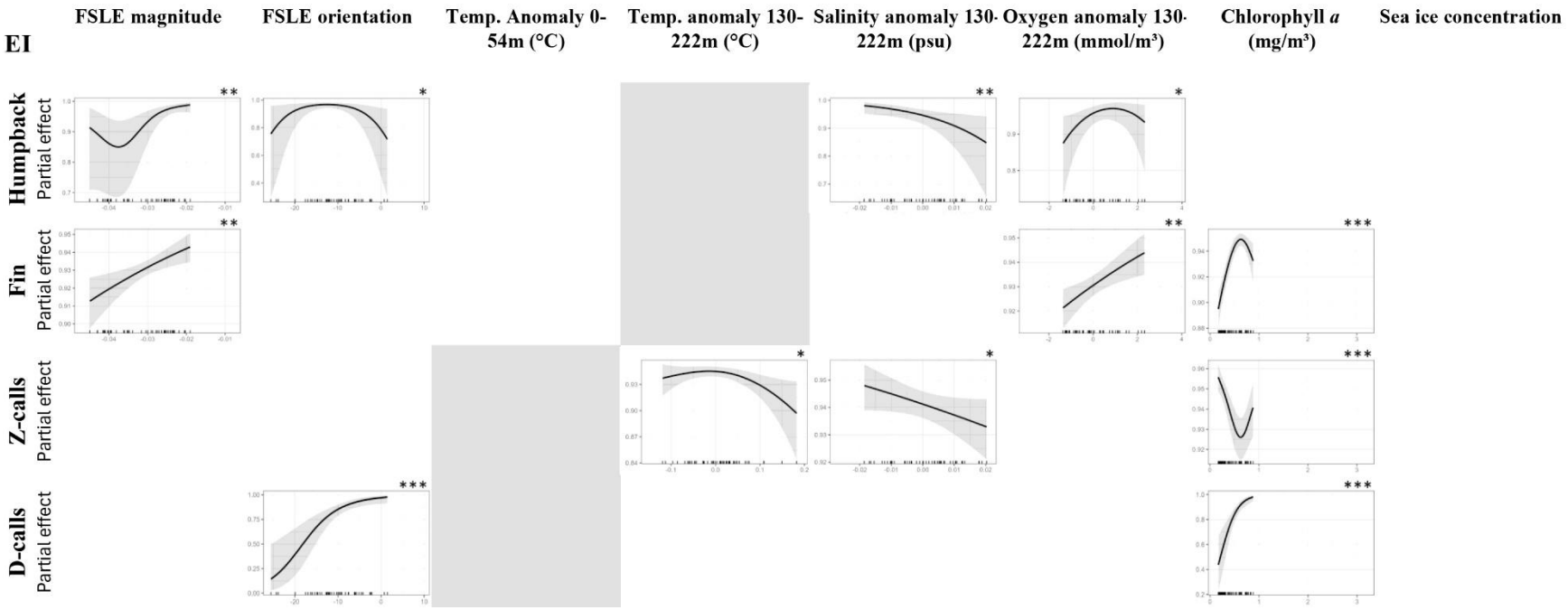
EI
FSLE magnitude
FSLE orientation
Temp. Anomaly 0-54m (°C)
Temp. anomaly 130-222m (°C)
Salinity anomaly 130-222m (psu)
Oxygen anomaly 130-222m (mmol/m³)
Chlorophyll a (mg/m³)
Sea ice concentration
Humpback
Fin
Z-calls
D-calls
Partial effect

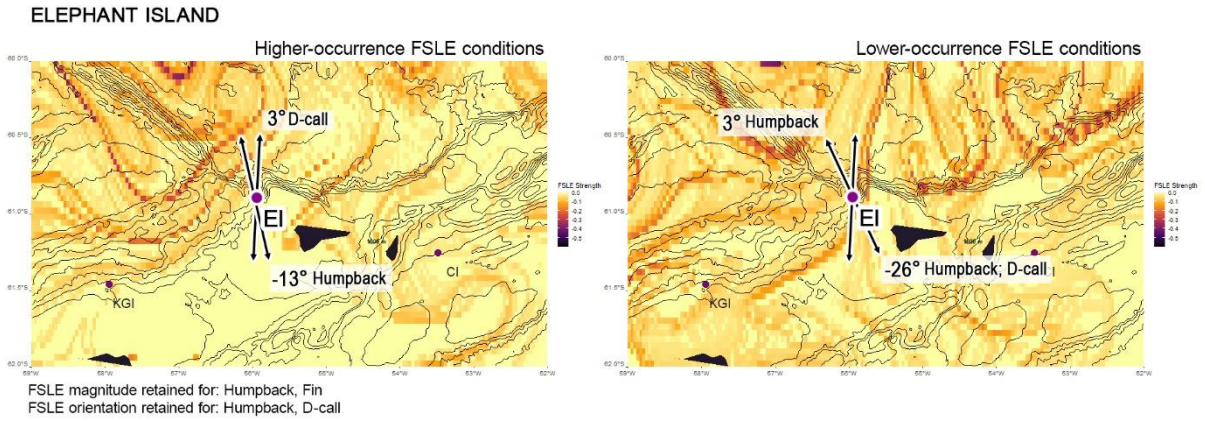

Figure 9. Representation of FSLE conditions associated with baleen whale acoustic occurrence at Elephant Island. Background shading shows representative backward-in-time finite-size Lyapunov exponent (FSLE) fields selected from periods when FSLE magnitude at the Elephant Island recording site corresponded to values associated with relatively higher (left) and lower (right) modeled acoustic occurrence based on the GAM smooths. More negative (darker) FSLE values indicate stronger convergence. Black contours show bathymetry at 500 m intervals, black shapes indicate land, and purple points mark the Elephant Island (EI), King George Island (KGI), and Clarence Island (CI) recording sites. FSLE magnitude was retained in the final humpback and fin whale models at Elephant Island; therefore, FSLE magnitude representation in this figure pertains only to them. Arrows originating at the Elephant Island site indicate FSLE orientation values associated with modeled acoustic occurrence for humpback whales and blue whale D-calls, the two response types for which FSLE orientation was retained. Angle labels indicate orientation relative to the north-south axis. Representative magnitudes and orientations were selected based on the peaks and troughs of the relevant GAM smooths and their approximate corresponding FSLE value.

3.3.2. King George Island

The humpback whale model explained 47% of the deviance at King George Island (Table 1). Humpback whale calls were significantly associated with FSLE magnitude ($p < 0.001$), chlorophyll *a* ($p < 0.001$), and sea ice concentration ($p < 0.001$; Table 1). Acoustic occurrence declined as FSLE values became less negative (Figures 10 and 11). Chlorophyll *a* showed a positive relationship, with occurrence increasing rapidly at a lower chlorophyll *a* concentration before reaching a plateau at a higher concentration (Figure 10). Sea ice concentration had a similar relationship; occurrence initially increased with increasing ice concentration, but changed comparatively little across the upper portion of the observed range (Figure 10).

The fin whale 20 Hz model explained 69% of the deviance at King George Island (Table 1). Fin whale acoustic occurrence was significantly associated with FSLE magnitude ($p < 0.001$), chlorophyll *a* ($p < 0.001$), temperature anomaly between 0-54 m ($p = 0.005$), and sea ice concentration ($p < 0.001$; Table 1). Acoustic occurrence increased with FSLE magnitude toward an intermediate optimum and then declined slightly at the least negative FSLE values (Figures 10 and 11). Occurrence showed a negative relationship with chlorophyll *a* concentration, with the steepest decline occurring in the central portion of the observed range (Figure 10). Occurrence increased under cooler-than-seasonal temperatures in the upper water column and decreased with increasing ice concentration (Figure 10).

The blue whale Z-call model explained 32% of the deviance at King George Island (Table 1). Z-calls were significantly associated with chlorophyll *a* ($p < 0.001$) and oxygen anomaly between 130-222 m ($p = 0.006$; Table 1). Acoustic occurrence generally declined as chlorophyll *a* concentration increased; a small increase was observed at the highest

concentration, but uncertainty was greater at this end of the observed range (Figure 10). Oxygen anomaly showed an intermediate optimum, with the greatest occurrence being at moderately positive anomalies and lower occurrence at the lowest and highest anomalies (Figure 10). However, the decrease at the highest end of the observed range coincides with greater uncertainty (Figure 10).

The blue whale D-call model explained 41% of the deviance at King George Island (Table 1). D-call occurrence was significantly associated with FSLE magnitude ($p < 0.001$), FSLE orientation ($p < 0.001$), chlorophyll *a* ($p < 0.001$), and temperature anomaly between 130-222 m ($p = 0.001$; Table 1). Occurrence increased as FSLE values became less negative and decreased as FSLE orientation values increased (Figures 10 and 11). D-call occurrence increased as deep temperature anomaly became more positive (Figure 10). An intermediate optimum was seen with chlorophyll *a* concentration, with lower occurrence at both the highest and lowest ends of the observed range (Figure 10). However, uncertainty was greater near the high end of the range (Figure 10).

Figure 10. Estimated partial effects of environmental predictors retained in final generalized additive models (GAMs) for baleen whale acoustic occurrence at King George Island.

Rows represent, from top to bottom, humpback whale calls, fin whale 20 Hz calls, blue whale Z-calls, and blue whale D-calls. Columns represent the environmental predictors considered during the modeling process. Black curves show the estimated partial effect of each retained predictor, shaded bands indicate 95% confidence intervals, and the rug marks along the x-axis indicate the distribution of observed predictor values. Asterisks indicate smooth-term significance ($p \leq 0.05$*, $p \leq 0.01$**, $p \leq 0.001$***). Gray cells indicate predictors excluded during the pre-selection process, whereas empty white cells indicate predictors that passed pre-selection but were not retained in the final model. Predictor x-axis limits are held constant for each variable across Figures 8, 10, and 12 and span the combined range across sites to facilitate comparison. Y-axis limits vary between smooths.

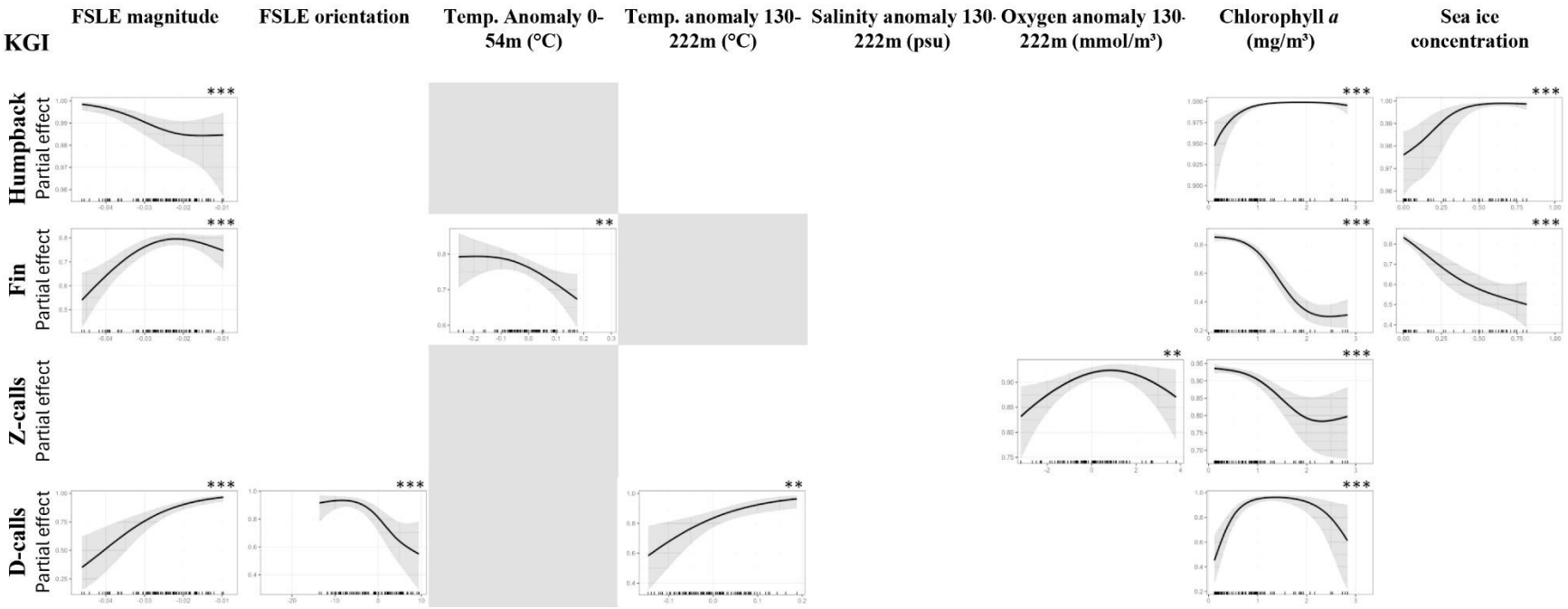
KGI
FSLE magnitude
FSLE orientation
Temp. Anomaly 0-54m (°C)
Temp. anomaly 130-222m (°C)
Salinity anomaly 130-222m (psu)
Oxygen anomaly 130-222m (mmol/m³)
Chlorophyll a (mg/m³)
Sea ice concentration
Humpback
Fin
Z-calls
D-calls
Partial effect

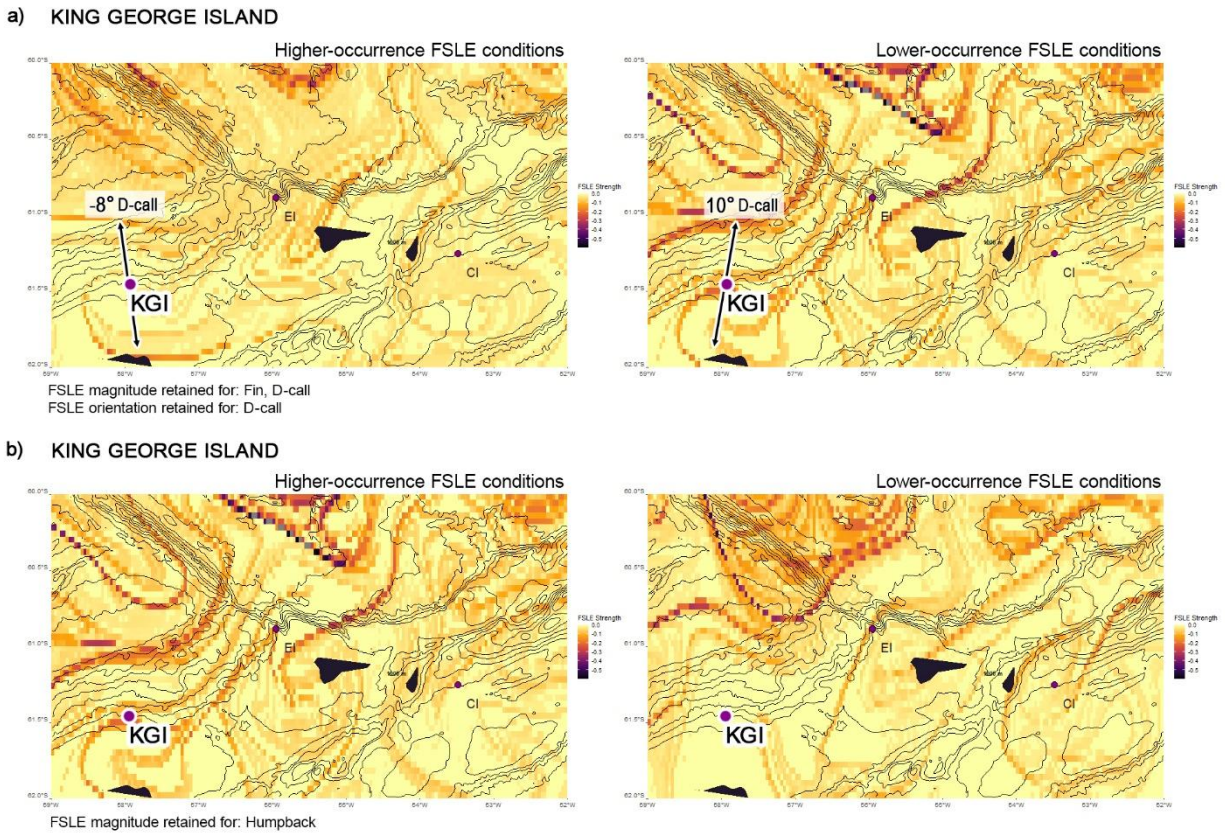

Figure 11. Representation of FSLE conditions associated with baleen whale acoustic occurrence at King George Island. Background shading shows representative backward-in-time finite-size Lyapunov exponent (FSLE) fields selected from periods when FSLE magnitude at the King George Island recording site corresponded to values associated with relatively higher (left) and lower (right) modeled acoustic occurrence based on the GAM smooths. More negative (darker) FSLE values indicate stronger convergence. Black contours show bathymetry at 500 m intervals, black shapes indicate land, and purple points mark the Elephant Island (EI), King George Island (KGI), and Clarence Island (CI) recording sites. (a) Higher- and lower-occurrence FSLE conditions for fin whale 20 Hz calls and blue whale D-calls, which showed broadly similar relationships with FSLE magnitude. Arrows originating at the King George Island site indicate FSLE orientation values associated with relatively higher (left) and lower (right) blue whale D-call occurrence, the response type for which FSLE orientation was retained. Angle labels indicate orientation relative to the north-south axis. (b) Higher- and lower-occurrence FSLE conditions for humpback whale calls, shown separately because their modeled relationship with FSLE magnitude differed from those of fin whales and blue whale D-calls at King George Island. FSLE orientation was not retained for humpback whales at King George Island and is therefore not illustrated. Representative magnitudes and orientations were selected based on the peaks and troughs of the relevant GAM smooths and their approximate corresponding FSLE value.

3.3.3. Clarence Island

The humpback whale model explained 39% of the deviance at Clarence Island (Table 1). Humpback whale acoustic occurrence was significantly associated with FSLE magnitude ($p < 0.001$), chlorophyll *a* ($p < 0.001$), salinity anomaly between 130-222 m ($p = 0.005$), temperature anomaly between 0-54 m ($p = 0.03$), and sea ice concentration ($p = 0.04$; Table 1). FSLE magnitude showed an intermediate optimum, with lower occurrence at both ends of the observed range (Figures 12 and 13). Humpback whale occurrence declined as shallow water temperature anomaly became more positive (Figure 12). An overall positive relationship was seen with deep salinity anomaly, with acoustic occurrence rapidly increasing at the lower end of the observed range before plateauing; however, uncertainty at this low end was greater (Figure 12). The opposite relationship was seen with chlorophyll *a* concentration, where occurrence stayed stable at a lower concentration and declined at a higher concentration, though once again, uncertainty was greater at the higher end of the observed range (Figure 12). Sea ice concentration showed a U-shaped relationship, with occurrence decreasing as ice concentration increased before increasing once again at a higher concentration (Figure 12). However, uncertainty was greater at these higher sea ice concentrations (Figure 12).

The fin whale 20 Hz model explained 48% of the deviance at Clarence Island (Table 1). Fin whale acoustic occurrence was significantly associated with FSLE magnitude ($p < 0.001$), oxygen anomaly between 130-222 m ($p < 0.001$), and salinity anomaly between 130-222 m ($p < 0.001$; Table 1). FSLE magnitude showed an intermediate optimum at moderately high values (Figures 12 and 13). Deep oxygen anomaly also showed an intermediate optimum near the middle of the observed range, and deep salinity anomaly showed a U-shaped relationship,

with acoustic occurrence increasing at both the most negative and most positive salinity anomalies (Figure 12).

The blue whale Z-call model explained 33% of the deviance at Clarence Island (Table 1). Z-call occurrence was significantly associated with FSLE magnitude ($p = 0.009$), oxygen anomaly between 130-222 m ($p < 0.001$), and temperature anomaly between 130-222 m ($p = 0.009$; Table 1). FSLE magnitude exhibited an intermediate optimum at moderately high values (Figures 12 and 13). Z-calls were negatively associated with deep temperature anomaly (Figure 12). Deep oxygen anomaly showed an intermediate optimum (Figure 12).

The blue whale D-call model explained 58% of the deviance at Clarence Island (Table 1). D-calls were significantly associated with FSLE magnitude ($p < 0.001$), chlorophyll *a* ($p < 0.001$), temperature anomaly between 130-222 m ($p = 0.009$), and sea ice concentration ($p = 0.02$; Table 1). FSLE magnitude showed an intermediate optimum at moderately high values (Figures 12 and 13). D-call occurrence had a positive relationship with deep temperature anomaly (Figure 12). D-calls increased steeply with chlorophyll *a* concentration at the lower end of the observed range before reaching a plateau (Figure 12). Sea ice concentration showed an intermediate optimum at moderately low concentrations (Figure 12).

Figure 12. Estimated partial effects of environmental predictors retained in final generalized additive models (GAMs) for baleen whale acoustic occurrence at Clarence Island.

Rows represent, from top to bottom, humpback whale calls, fin whale 20 Hz calls, blue whale Z-calls, and blue whale D-calls. Columns represent the environmental predictors considered during the modeling process. Black curves show the estimated partial effect of each retained predictor, shaded bands indicate 95% confidence intervals, and the rug marks along the x-axis indicate the distribution of observed predictor values. Asterisks indicate smooth-term significance ($p \leq 0.05$*, $p \leq 0.01$**, $p \leq 0.001$***). Gray cells indicate predictors excluded during the pre-selection process, whereas empty white cells indicate predictors that passed pre-selection but were not retained in the final model. Predictor x-axis limits are held constant for each variable across Figures 8, 10, and 12 and span the combined range across sites to facilitate comparison. Y-axis limits vary between smooths.

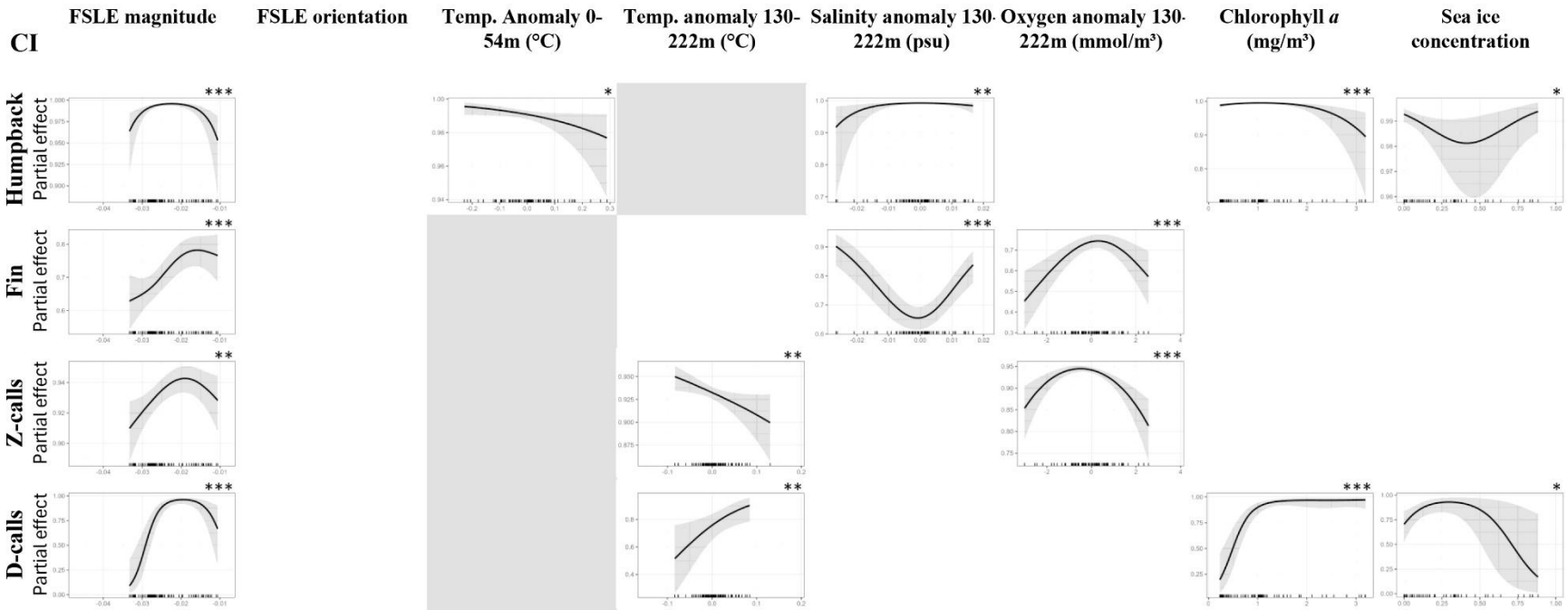
CI
FSLE magnitude
FSLE orientation
Temp. Anomaly 0-54m (°C)
Temp. anomaly 130-222m (°C)
Salinity anomaly 130-222m (psu)
Oxygen anomaly 130-222m (mmol/m³)
Chlorophyll a (mg/m³)
Sea ice concentration
Humpback
Fin
Z-calls
D-calls
Partial effect

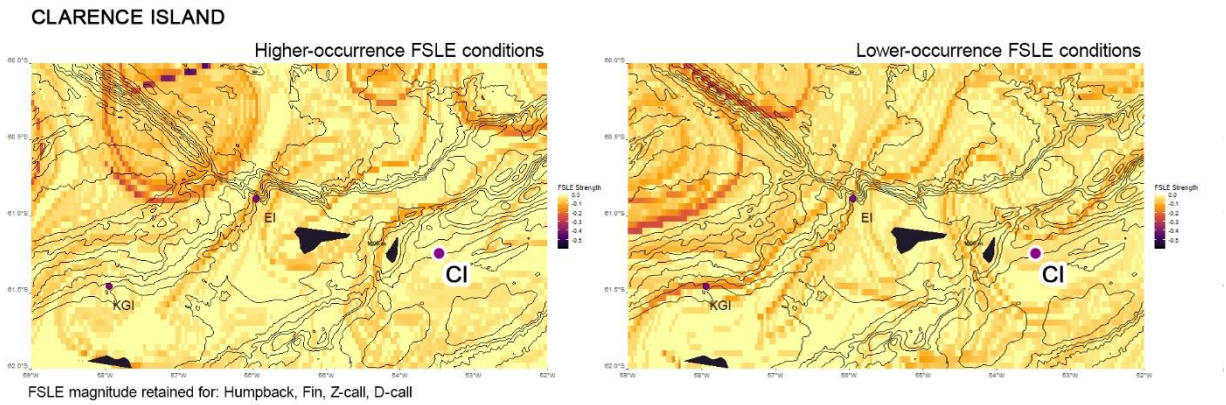

Figure 13. Representation of FSLE conditions associated with baleen whale acoustic occurrence at Clarence Island. Background shading shows representative backward-in-time finite-size Lyapunov exponent (FSLE) fields selected from periods when FSLE magnitude at the Clarence Island recording site corresponded to values associated with relatively higher (left) and lower (right) modeled acoustic occurrence based on the GAM smooths. More negative (darker) FSLE values indicate stronger convergence. Black contours show bathymetry at 500 m intervals, black shapes indicate land, and purple points mark the Elephant Island (EI), King George Island (KGI), and Clarence Island (CI) recording sites. FSLE magnitude was retained in all four final Clarence Island models (humpback whale calls, fin whale 20 Hz calls, blue whale Z-calls, and blue whale D-calls), which showed broadly similar relationships to FSLE magnitude. FSLE orientation was not retained in any final Clarence Island models and therefore is not illustrated. Representative magnitudes were selected based on the peaks and troughs of the relevant GAM smooths and their approximate corresponding FSLE value.

3.3.4. Model diagnostics

Diagnostic evaluation indicated that all twelve final GAMs converged successfully, with positive-definite Hessians and full model rank. Simulated quantile-quantile plots generally showed agreement between observed residuals and the distribution expected under the fitted Tweedie models. Departures were concentrated primarily near the extremes and were most evident in the humpback whale models across all three sites, with smaller or isolated departures in several other models. No clear pattern was evident with respect to site or the number of predictors retained in the final model. Residual histograms and plots of residuals against the linear predictor similarly did not reveal a consistent pattern of strong model misspecification across sites or acoustic response types. Basis-dimension checks were satisfactory for most smooth terms. However, low k-index values were identified for several predictors, primarily in models from King George Island, indicating that some smooth terms may have retained residual structure not fully represented by the specified basis dimension. These results were interpreted cautiously because the effective degrees of freedom of the affected smooths were generally below the maximum allowed by the specified basis dimension.

Residual temporal autocorrelation was reduced by the site-specific temporal binning procedure but was not completely eliminated in all models. Little remaining autocorrelation was evident in most Elephant and Clarence Island models, although some residual structure remained for the Elephant Island blue whale Z-call and Clarence Island fin whale models. More residual autocorrelation remained in the King George Island models. Consequently, statistical significance and environmental relationships from models exhibiting residual temporal structure should be interpreted with some additional caution.

Overall, the diagnostic results did not indicate pervasive departures from the assumed response distribution or systematic residual patterns across the models. However, remaining temporal autocorrelation and basis-dimension diagnostic flags represent limitations of the final models and should be considered when interpreting individual environmental associations.

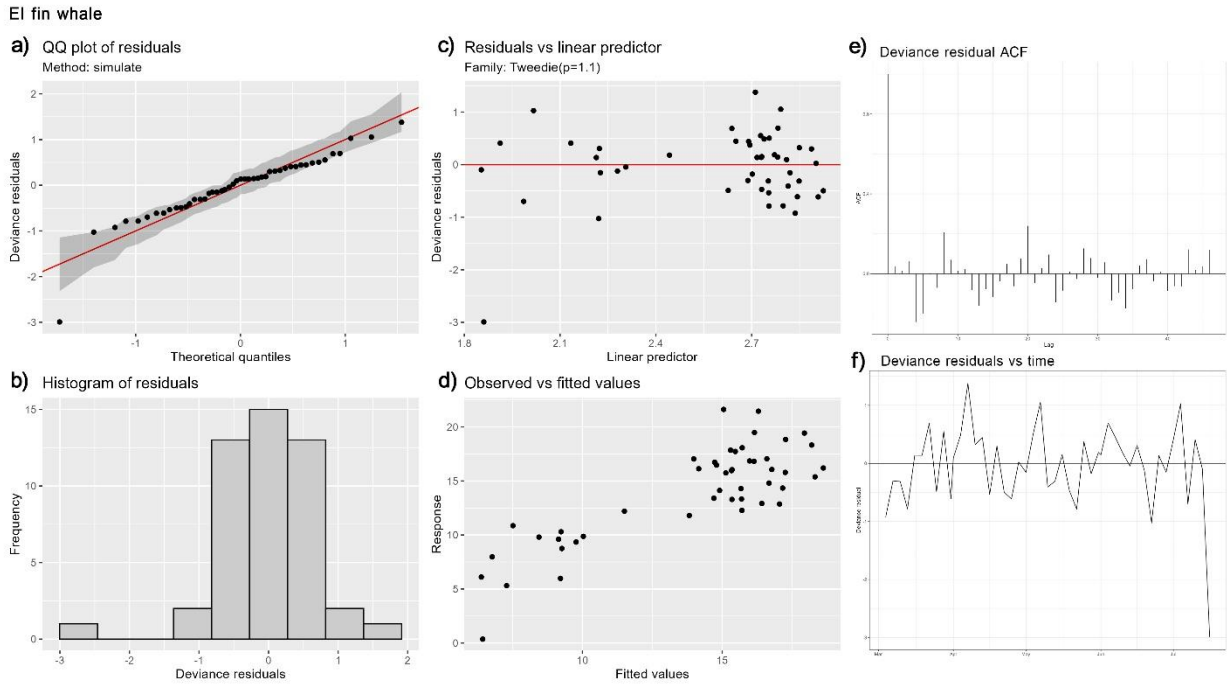

Figure 14. Diagnostic plots for the final generalized additive model (GAM) of fin whale 20 Hz acoustic occurrence at Elephant Island. (a) Simulation-based quantile-quantile (Q-Q) plot of deviance residuals, with the red line showing the expected relationship and the dark gray region representing the simulation envelope; (b) histogram of deviance residuals; (c) deviance residuals plotted against the linear predictor, with the red horizontal line indicating zero; (d) observed versus fitted response values; (e) autocorrelation function (ACF) of deviance residuals; and (f) deviance residuals through time. This model was selected as an example of comparatively good diagnostic performance, with generally close agreement in the Q-Q plot, little systematic residual structure, and relatively little remaining temporal autocorrelation.

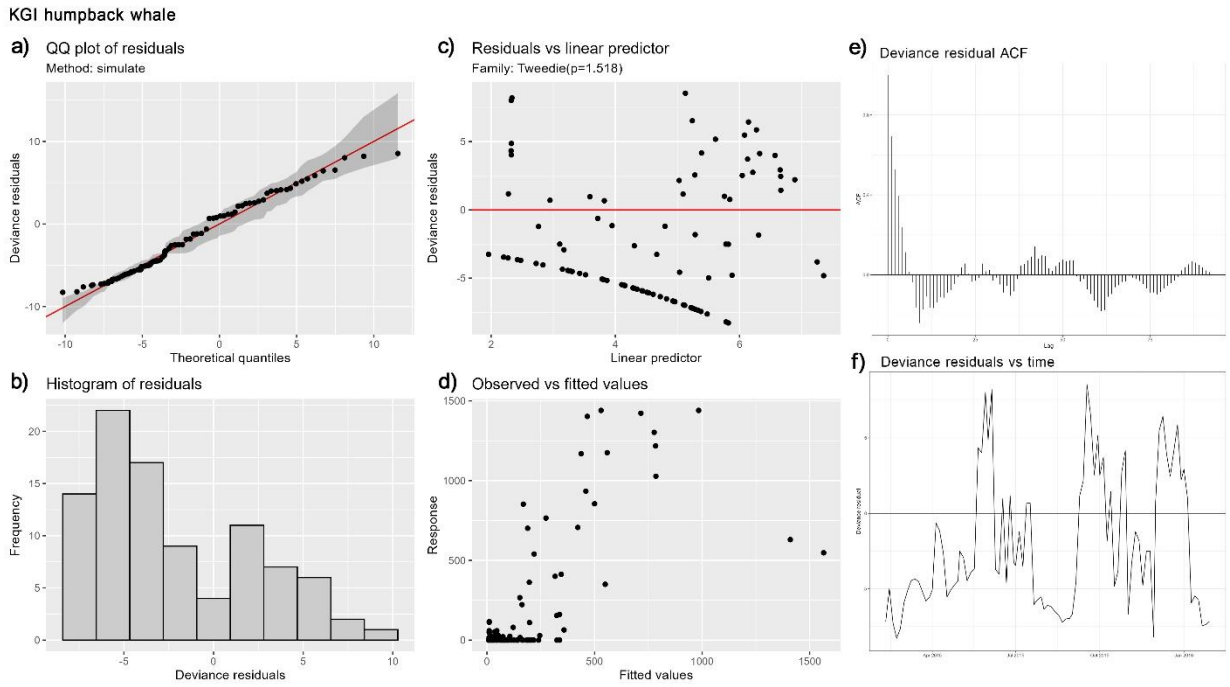

Figure 15. Diagnostic plots for the final generalized additive model (GAM) of humpback whale acoustic occurrence at King George Island. (a) Simulation-based quantile-quantile (Q-Q) plot of deviance residuals, with the red line showing the expected relationship and the dark gray region representing the simulation envelope; (b) histogram of deviance residuals; (c) deviance residuals plotted against the linear predictor, with the red horizontal line indicating zero; (d) observed versus fitted response values; (e) autocorrelation function (ACF) of deviance residuals; and (f) deviance residuals through time. This model was selected to illustrate greater diagnostic limitations within the final model set, including departures in the tails of residual distribution and remaining temporal autocorrelation.

DISCUSSION

4.1. OVERVIEW

Across acoustic response types and sites, the models revealed both recurring environmental relationships and substantial variation in how baleen whale acoustic occurrence is associated with local oceanography. When considered together, these results suggest that baleen whale acoustic occurrence around the northern South Shetland Islands was associated with a dynamic combination of physical and biological processes rather than with a single set of favorable environmental conditions. The repeated retention of mesoscale structure and subsurface anomalies suggests that processes controlling water mass transport, mixing, and potentially prey aggregation may contribute to the observed patterns of acoustic occurrence. The frequency of nonlinear relationships further supports this interpretation, as acoustic occurrence was often greatest at intermediate conditions or across particular portions of the observed range, rather than simply increasing or decreasing with a predictor.

The substantial variation among sites, species, and call types also indicates that the whales may not use this shared krill-based ecosystem in identical ways. Differences in their responses to a set of predictors may reflect species-specific prey preferences, habitat selection, migration patterns, and behavioral context. Rather than identifying a universal definition of ideal baleen whale habitat, these models suggest that suitable habitat emerges from the interactions between oceanographic structure, water mass influence, and species-specific ecology.

4.2. PATTERNS IN ACOUSTIC PRESENCE

Several acoustic occurrence patterns emerged across and between sites, with each call type showing some broadly similar temporal characteristics across the three sites and years

(Figures 4a-d). However, analysis of these patterns across sites is limited by the recording time differences; recording at Elephant Island only took place for approximately four months; this provides only a small snapshot of the year and cannot reveal seasonal trends.

Fin whale calling followed the most consistent seasonal trend, peaking around April at all sites, though it cannot be determined whether the decrease in acoustic occurrence at the end of the Elephant Island deployment continues as the year progresses (Figure 4b). This strong seasonality of fin whale 20 Hz calls has been noted repeatedly in the literature. Burkhardt et al. (2021) found that 20 Hz calling at Elephant Island began in February and declined in August. Širović et al. (2004), at several sites around the Antarctic Peninsula, recorded fin whale calls primarily from February through July, with a peak in May; however, they did not detect any fin whale calls between July and January. While this overall seasonal trend is consistent with our results, we did detect calls year-round, though at a far lower level (Figure 4b). The daily call index value for fin whales was higher more often at Elephant Island than at the other two sites (Figure 4b). Elephant Island is a known feeding ground for aggregations of fin whales, and is typically considered one of their most important habitats in the region (Burkhardt et al., 2021; Panigada et al., 2024).

As with these results, the literature supports the year-round presence of blue whales in the Southern Ocean based on Z-calls, indicating a less traditional migration pattern (Širović et al., 2004, 2009; Smith et al., 2024; Thomisch et al., 2016). Širović et al. (2009) suggest that a staggered migration in Antarctic blue whales could explain the occurrence of year-round calls. It is also possible that some individuals do not participate in a yearly migration and instead overwinter in Antarctic waters (Smith et al., 2024; Thomisch et al., 2016). This is consistent with our results, which show sustained Z-calling throughout the year (Figure 4c).

Unlike Z-calls, D-calls did not show a continuous trend and instead occurred in short, intense bursts (Figure 4d). Notably, the strongest peaks in D-call occurrence at King George and Clarence Islands occurred at similar times of the year, despite the sites being recorded in different years (Figure 4d). This could possibly suggest a repeating, seasonal association for D-calls in this region; however, additional years of data would be necessary to establish this pattern. D-calls at Elephant Island were few and far between, making a pattern difficult to interpret (Figure 4d). While these short, occasional peaks in calling at these times of year are not described in the literature, it has been reported that D-calls are overall more temporally restricted than Z-calls (Miller et al., 2024; Shabangu et al., 2020). D-calls are thought to be associated with foraging behavior and can be produced by both males and females, while Z-calls are produced only by males (McDonald et al., 2006; Oleson et al., 2007). These brief periods of elevated D-calling may reflect increases in foraging or social activity, rather than changes in blue whale presence.

Seasonal patterns in these results were less consistent for humpback whales. At King George Island, acoustic occurrence increased substantially from approximately September through January, consistent with the seasonal movement of humpback whales into Antarctic feeding grounds during the spring and summer (Johannessen et al., 2022; Thiele et al., 2004; Figure 4a). However, clear seasonal patterns were not evident at Elephant or Clarence Islands. At Elephant Island, few humpback whale vocalizations were recorded, and the relatively short deployment limits interpretation of broader seasonal trends (Figure 4a). Clarence Island showed a different pattern, with discrete peaks in acoustic occurrence separated by periods of relatively little calling throughout the year (Figure 4a). Although such a consistently repeating pattern does not appear to have been described, similarly episodic occurrence has been reported elsewhere in

Antarctica. Van Opzeeland et al. (2013) found that humpback whale calls occurred in bouts lasting 2-42 consecutive days, with calling occurring during both summer and winter, while Schall et al. (2020) documented pronounced periods of acoustic occurrence separated by intervals of sporadic detections. Thus, the episodic nature of humpback whale acoustic occurrence at Clarence Island may reflect short-term variation in habitat use or social activity, rather than seasonal migration trends. The occurrence of several peaks during winter months is also consistent with increasing evidence that a portion of the humpback whale population may overwinter in Antarctica (Clarke et al., 2026; Van Opzeeland et al., 2013).

4.3. SPECIES-SPECIFIC ASSOCIATIONS AND POTENTIAL NICHE PARTITIONING

Although several environmental predictors and trends were shared across species, the models and acoustic time series also revealed substantial differences between the four acoustic response types. This is particularly apparent for humpback and fin whales, which may overlap extensively throughout this Antarctic habitat. Horizontal niche partitioning between these species has previously been demonstrated around the Antarctic Peninsula. Herr et al. (2016) found distinct spatial distributions during whale and krill surveys; fin whales were concentrated along the shelf edge of the South Shetland Islands in the Drake Passage, while humpback whales were found predominantly within the Bransfield Strait. The dominant prey species also differed between these zones. Humpback whales were found in areas with greater *Euphausia superba* biomass, while fin whales fed in an area more dominated by *Thysanoessa macrura* (Herr et al., 2016). Santora et al. (2010) also examined the differences in krill length and maturity classes in relation to humpback and fin whale occurrence. They found that humpback whales were

associated with aggregations of smaller, juvenile krill, while fin whales were associated with larger, mature krill (Santora et al., 2010).

While research on niche partitioning involving blue whales is less extensive than for fin and humpback whales, blue whales have been reported to feed on smaller krill than fin whales (Laws, 1977). Additionally, historical stable-isotope analysis suggests differences in Antarctic blue and fin whales' migratory and foraging patterns; Smith et al. (2024) found evidence suggesting that some blue whales may be year-round residents in the Southern Ocean, while fin whales appear to migrate annually. They also found isotopic differences that could result from the two species feeding in different locations within the broader region, with fin whales feeding farther from the pack ice than blue whales (Smith et al., 2024). Though these isotopic results reflect these whales' ecology before their recovery from whaling, they may still be relevant to contemporary blue and fin whale populations.

Many patterns in the present study are consistent with species-specific habitat use, although these results cannot directly demonstrate niche partitioning. Humpback and fin whale models often retained different predictors or showed different responses to the same predictor, particularly at King George Island (Figure 10, Table 1). While evidence of partitioning at Elephant and Clarence Islands is less clear, it may still be influencing the results at these sites. At King George Island, humpback whale acoustic occurrence was associated with stronger FSLE values, increasing chlorophyll, and increasing sea ice, while these relationships were reversed for fin whales (Figure 10).

The acoustic time series suggest that there may be an additional temporal component to these whales' differences in habitat use. At King George Island, fin whale calling was strongest from approximately March through June and declined later in the year, while humpback whale

calling was comparatively low during much of this period, becoming stronger later in the deployment (Figure 4a and 4b). The contrast seen at all sites between the seasonality of fin whale calling and the consistency of blue whale Z-calls supports the historical evidence from Smith et al. (2024) that migratory patterns differ between the species (Figures 4b and c).

Because these whales may be associated with different species and size classes of krill, or may be foraging at different times of the year, the results should not necessarily be interpreted as indicating which conditions are favorable for krill in general. The favorability of a given set of environmental conditions likely differs depending on the species, size, and maturity of krill. Therefore, the results may instead indicate which conditions are favorable for a given whale species' preferred type of krill, at the time of year in which they forage. This cannot, however, be verified without direct measurements of krill.

4.4. MESOSCALE CIRCULATION AND FSLE STRUCTURE

The consistency with which FSLE variables were retained across models provides some evidence that mesoscale oceanographic structure was associated with baleen whale acoustic occurrence near the South Shetland Islands during these deployments. Backward-in-time FSLE measures identify attracting or converging structures and can be used to identify Lagrangian structures, including frontal and eddy boundaries that can indicate the movement and mixing of water parcels (d'Ovidio et al., 2004).

There are multiple mechanisms by which these features could influence whales. Convergence zones can transport, concentrate, or retain phytoplankton and zooplankton (d'Ovidio et al., 2010). They also represent boundaries and mixing zones between water masses with different properties, some of which may be more favorable to prey than others. The

relevance of these mesoscale structures to baleen whales has been demonstrated in other environments; Fahlbusch et al. (2024) found that aggregative Lagrangian coherent structures were associated with increased krill density and baleen whale occurrence in the California Current. In the Antarctic Peninsula, Nowacek et al. (2011) documented extremely dense aggregations of humpback whales and krill in a retentive circulation feature in Wilhelmina Bay, emphasizing the ecological importance of aggregation and retention.

However, the models from the South Shetland Islands do not indicate an overwhelming association with the strongest convergence. Rather, many models show that acoustic occurrence increases towards lower and intermediate convergence strength (Figures 8, 10, and 12). While strong convergence zones may aggregate krill, these same structures may also advect krill out of the area. Based on these results, it appears possible that weaker FSLE magnitudes could be more favorable for krill retention near the South Shetland Islands than in other systems; however, this mechanism cannot be tested without direct measurements of krill retention. Additionally, though retention alone may be important, the association with weaker FSLE magnitudes may be a consequence of preferred krill habitat being in the water mass behind or in front of a given convergence zone. The strongest FSLE values identify the cores of attracting structures, but biologically favorable conditions may occur adjacent to these structures rather than directly along the strongest ridge. FSLE ridges mark the boundaries between water parcels with different origins and properties that may be more or less favorable to krill.

The main deviation from this pattern was with humpback whales at King George Island, where acoustic occurrence increased at more negative (stronger) FSLE values (Figures 10 and 11b). The optimum values for humpback whales at Clarence Island also encompassed more negative values than the other call types (Figure 12). While the retention of some krill patches

may favor lower convergence strength, stronger convergence, as seen in other systems, likely does not indicate an absence of krill. Rather, this may be an indication of humpback whales taking advantage of different size classes or species of krill, which could respond differently to mesoscale features (Herr et al., 2016).

FSLE orientation was significant in fewer models than FSLE magnitude; however, it was still retained in the D-call model at King George Island and the humpback whale and D-call models at Elephant Island (Figures 8 and 10). Unlike with magnitude, the ecological meaning of FSLE orientation is inherently dependent on bathymetry. Circulation around the northern Antarctic Peninsula is strongly influenced by bathymetry, with shelf breaks and slopes affecting the transport pathways for water, nutrients, and potentially krill (Jiang et al., 2013; Thompson et al., 2009). Consequently, the alignment of an FSLE ridge relative to local bathymetry may affect whether it promotes along-slope transport, cross-slope transport, or local retention. Because bathymetry differs substantially between the three sites, the same FSLE orientation would not necessarily have the same ecological meaning at each location. At King George Island, D-call occurrence was associated with FSLE orientations being slightly more perpendicular to the slope (Figure 11). At Elephant Island, the complicated bathymetry and differences between species make it difficult to find patterns between FSLE orientation and bathymetry (Figure 9).

4.5. SUBSURFACE VARIABLES AND WATER MASS INFLUENCE

Temperature, salinity, and oxygen anomalies can act as indicators of water masses, though in systems like the northern Antarctic Peninsula, where water mass and current interactions are extremely complex, it is often difficult to confidently assign a pattern in these variables to one water mass (García et al., 2002; Loeb et al., 2010; Patterson & Sievers, 1980;

Sangrà et al., 2011; Tokarczyk, 1987). The region lies at the intersection of several currents and water sources, including relatively warm and fresh Transitional Zonal Water with Bellingshausen influence, colder, more saline Transitional Zonal Water with Weddell Sea influence, and warmer, more saline Circumpolar Deep Water, along with several other interacting currents and water masses from the Drake Passage, Bransfield Strait, Weddell Sea, and Scotia Sea (García et al., 2002; Loeb et al., 2010; Patterson & Sievers, 1980; Sangrà et al., 2011). When the relative influence and mixing of these waters change, concurrent anomalies in temperature, salinity, and dissolved oxygen can be observed. Such variability has previously been linked to changes in phytoplankton and zooplankton communities and to krill recruitment in this region (Loeb et al., 2010). Therefore, the significance of these anomalies in the GAM results may not suggest an independent association for one variable, but instead may function as indicators of changing water masses that alter the distribution or suitability of krill habitat.

The repeated importance of temperature, salinity, and dissolved oxygen anomalies, particularly within the 130-222 m depth range, suggests that subsurface oceanographic variability may be associated with baleen whale occurrence, which is intuitive given that this depth band is known to encompass ecologically relevant subsurface prey habitat (Miller et al., 2019). Because these variables were deseasoned relative to a 10-year baseline, they represent deviations from the seasonal norm, rather than the expected progression of the seasonal cycle. Deseasoning reduces the contribution of the mean seasonal cycle, allowing the models to evaluate whether departures from climatological conditions were associated with acoustic occurrence. It does not necessarily remove all seasonal covariance or isolate causal effects. When anomalies in these variables occur, they can indicate that a shift has occurred in the area's dominant water mass. Some of these water masses are likely to be more favorable to

krill, and may already contain aggregations of krill that are transported into the area with the water mass.

4.6. CHLOROPHYLL *a*

Chlorophyll *a* was the second most commonly retained predictor, being significant in nine of the twelve final models (Table 1). Chlorophyll *a* is a proxy measurement for phytoplankton, which provide a food source for krill. However, the final models show a complex relationship between chlorophyll *a* concentration and acoustic occurrence, varying among sites and acoustic response types (Figures 8, 10, and 12). The variation in these relationships likely stems from the fact that chlorophyll is not a direct measurement of krill.

It is also important to note that the chlorophyll variable used in these models was not deseasoned. Therefore, it may also be capturing a seasonal trend, and differences between species may be more related to phenological differences in whale presence and acoustic behavior.

Fin whale and D-calls at Elephant Island, humpback whale and D-calls at King George Island, and D-calls at Clarence Island all showed an overall positive relationship between acoustic occurrence and chlorophyll *a* concentration (Figures 8, 10, and 12). A higher concentration of chlorophyll, and thus greater primary productivity, could support a higher krill concentration, which could in turn attract feeding whales. While the positive relationship between acoustic occurrence and chlorophyll is consistent at the lower end of the observed range, these models all exhibit a change towards higher chlorophyll concentrations, with the relationships either plateauing or turning more negative (Figures 8, 10, and 12). This may suggest that an increase in chlorophyll does not lead to an increase in krill once a certain

threshold is reached, as was found by Silk et al. (2016), where the relationship between chlorophyll and krill plateaued before maximum chlorophyll concentration was reached. However, direct measurements of krill would be necessary to evaluate this mechanism.

The remaining models for which chlorophyll was significant, Z-calls at Elephant Island, fin whales and Z-calls at King George Island, and humpback whales at Clarence Island, showed overall negative relationships between chlorophyll *a* and acoustic occurrence, though greater uncertainty at the higher end of the observed range makes it difficult to interpret the Clarence Island humpback whale model (Figure 12). While these negative relationships may seem counterintuitive, studies have demonstrated negative relationships between krill and chlorophyll; krill exerting top-down control on phytoplankton can reduce chlorophyll concentration as they graze, leading to a decrease in chlorophyll levels as krill aggregate and feed (Whitehouse et al., 2009).

The discrepancy between the negative relationship between fin whale acoustic occurrence and chlorophyll *a* at King George Island and the positive relationship at Elephant Island may be a result of the difference in recording times between the two sites. Elephant Island was recorded for approximately four months, capturing the autumn chlorophyll peak (Figure 5). Meanwhile, King George Island was recorded for nearly a year, and that deployment captured both the autumn chlorophyll peak and the substantially larger spring peak (Figure 6). The seasonality of the fin whale 20 Hz calls meant that calling peaked in autumn and declined towards spring (Figure 4b). This strong seasonal pattern in fin whale calling may be masking their relationship with chlorophyll when the entire year is considered, as at King George Island, rather than when only the months with strong fin whale calling were considered, as at Elephant Island.

When interpreting these relationships, it is also important to consider that measures of chlorophyll do not differentiate between types of phytoplankton. High chlorophyll concentration in an area could represent a type of phytoplankton that is not a food source for krill; krill are known to preferentially feed on diatoms and are also omnivorous (Haberman et al., 2003; Price et al., 1988). An additional source of complexity is the potential time lag between an increase in chlorophyll *a* and the aggregation of grazing krill. Chlorophyll *a* represents phytoplankton biomass at the time of observation, whereas krill may respond to food availability over longer timescales. Along the Antarctic Peninsula, a positive summer chlorophyll anomaly has been associated with stronger krill recruitment the following year, suggesting that there can be a substantial delay between the onset of a phytoplankton bloom and a response from krill (Saba et al., 2014). Trophic lags such as this have been proposed to explain nonlinear or weak relationships between chlorophyll and krill in the Southern Ocean (Harrison et al., 2020).

4.7. SEA ICE

Sea ice concentration was retained as a significant predictor in four models and showed different relationships between species and sites (Figures 8, 10, and 12, Table 1). At King George Island, humpback whale acoustic occurrence increased with ice concentration before reaching a plateau, while fin whale acoustic occurrence decreased as ice concentration increased (Figure 10). At Clarence Island, humpback whale acoustic occurrence showed a U-shaped response and blue whale D-calls peaked at an intermediate ice concentration (Figure 12). Sea ice was not significant in any of the Elephant Island models, which is consistent with the fact that the site had low ice cover at the time of recording.

Sea ice can influence baleen whales by changing habitat accessibility for these air-breathing animals, while also influencing the life history and distribution of krill. Sea ice provides habitat and food resources for larval krill during periods of low pelagic productivity and has been linked to winter survival and subsequent recruitment (Daly, 2004). Seasonal changes in ice may also be associated with the redistribution of krill between offshore, shelf, and nearshore habitats, and satellite-tagged humpback whales along the Western Antarctic Peninsula have shown progressively smaller home ranges and greater proximity to shore from summer into fall, a pattern interpreted as tracking the seasonal movement of krill toward nearshore habitats later in the feeding season (Curtice et al., 2015; Nicol, 2006). This seasonal coupling between ice conditions, prey distribution, and whale movements may help explain why sea ice relationships in the present study were species-specific and nonlinear rather than uniformly negative. In particular, the positive-to-plateau relationship for humpback whales at King George Island and the U-shaped relationship at Clarence Island may indicate that sea ice concentration is capturing changing seasonal prey conditions or habitat use rather than a direct preference for a certain ice concentration.

Previous studies along the Antarctic Peninsula found negative relationships between sea ice concentration and both blue and fin whale calling, with fin whale calls particularly seasonal and concentrated before extensive winter ice formation (Širović et al., 2004). The negative King George Island fin whale relationship observed here is consistent with this pattern. Humpback whales, however, may use productive marginal or transitional habitats associated with changing ice conditions, and their distributions can shift substantially over the Antarctic feeding season as krill distributions change (Curtice et al., 2015).

When interpreting these sea ice concentration relationships, however, it is important to note that, as the sea ice variable was not deseasoned, these trends may reflect seasonal presence or calling behavior as opposed to the pure effect of ice concentration. There is also greater uncertainty at higher ice concentrations where relatively little data exists, making the interpretation of trends at high concentrations difficult. Sea ice may also influence apparent acoustic occurrence by altering the acoustic environment around the recorders; sea ice cover has been found to change ambient sound levels in the Southern Ocean (Menze et al., 2017). Additionally, interactions between sound and the ice surface can alter transmission loss and effective detection range (Alexander et al., 2016). In the Arctic, modeling of low-frequency bowhead whale calls found substantially reduced detection probabilities under ice-covered conditions relative to open water (Jones et al., 2022). Therefore, some apparent relationships between sea ice concentration and acoustic occurrence may reflect changes in call detectability in addition to changes in whale presence and calling behavior.

4.8. LIMITATIONS AND FUTURE DIRECTIONS

Several limitations are important to consider when interpreting these results and hypothesizing about what ecological processes might be responsible for the observed relationships. First, the three sites were recorded during different years and for different lengths of time. Elephant Island was particularly limited, with acoustic data available for only approximately four months, restricting the ability to evaluate seasonal patterns comparable to those observed during the longer King George and Clarence Island deployments. Because the sites were not recorded simultaneously, interannual variability could also contribute to apparent differences between sites.

Additionally, passive acoustic monitoring measures acoustic activity rather than whale abundance. Changes in acoustic occurrence may reflect changes in the number of whales within acoustic range, changes in calling behavior, or both. Calling rates can vary with species, call type, behavior, season, and other factors, making acoustic detections an imperfect proxy for the number of animals present (Marques et al., 2013). Consequently, the relationships identified here should be interpreted as associations with acoustic occurrence rather than direct relationships to whale abundance.

The differing results between blue whale Z- and D-calls also emphasize that behavioral context matters when acoustic detections are used as a proxy for presence. While these results are interpreted in relation to feeding behavior, some calls are not associated with foraging and are instead used in other social contexts, such as the Z-call (McDonald et al., 2006; Oleson et al., 2007). Therefore, differences between Z- and D-call models may reflect differences in calling behavior as well as differences in whale distribution or habitat use.

The corrected D-call series, particularly at King George Island, also contains uncertainty associated with the estimation of true detections during unverified gaps. This uncertainty was not propagated into the final models and may contribute to uncertainty in the estimated D-call relationships.

There is also spatial uncertainty associated with matching acoustic detections to the environmental conditions surrounding each recorder. Environmental predictors represent spatial averages over a fixed region around each site, whereas the effective area sampled acoustically was not explicitly estimated and likely differed between call types. Detection distance depends on call frequency and source level as well as bathymetry, ambient noise, and other factors affecting propagation conditions (Mellinger et al., 2007; Širović et al., 2007). In the Southern

Ocean, Širović et al. (2007) demonstrated that low-frequency blue and fin whale calls can propagate over tens to hundreds of kilometers under favorable conditions, illustrating that a calling whale detected by a stationary recorder may not necessarily occupy the same spatial area represented by the averaged value of a given environmental variable. Differences in source characteristics and calling rates of different call types can also produce differences in detection range between them, meaning that the four acoustic response types may represent somewhat different spatial scales even when recorded by the same instrument.

Because whale calling, chlorophyll concentration, and sea ice all exhibit pronounced seasonal cycles, relationships involving the non-deseasoned predictors may partly reflect shared phenology rather than independent environmental effects. Consequently, chlorophyll and sea ice smooths should be interpreted as associations with the seasonal environmental state rather than as evidence of a direct response to either variable alone.

Finally, some nonlinear relationships were most pronounced near the extremes of the observed predictor ranges, where relatively few observations were available and model uncertainty was often greater. GAM smooths are estimated from the available observations, and uncertainty is therefore greater where relatively little data exists. Apparent peaks, reversals, or increases near the edges of the observed range should therefore be interpreted cautiously, particularly where confidence intervals widen and rug plots indicate limited data support. Greater emphasis should be placed on relationships occurring within well-sampled portions of the environmental range.

Ideally, future studies trying to replicate and refine these results should attempt to minimize differences between sites by recording simultaneously and for the same length of time, preferably for an entire year or longer to capture seasonal trends. Future work should also

characterize the detection ranges of the different call types under varying conditions, to better understand the spatial mismatch between recorded calls and averaged environmental variables. Lastly, incorporating direct measurements of krill into future studies would also provide clarity as to whether these observed relationships are affecting whale presence through the control of krill, or whether another explanation is more probable.

4.9. CONCLUSION

FSLE variables emerged as the most consistently retained environmental predictors of baleen whale acoustic occurrence across the 12 models, with FSLE magnitude, orientation, or both being retained in the majority of final models. However, the direction and shape of these relationships varied between sites and acoustic response types, as did associations with chlorophyll *a*, subsurface anomalies, and sea ice. This variability suggests that acoustic occurrence was not associated with a single, consistent set of environmental conditions across species, call types, and site-year deployments, but instead emerged from interactions between physical water transport, water masses, primary production, and species- or behavior-specific habitat use. The contrasting responses observed among humpback, fin, and blue whale acoustic signals further emphasize that shared reliance on Antarctic krill does not imply identical use of the same environmental features. Resolving the mechanisms underlying these associations will require concurrent, long-term recording and direct, fine-scale measurements of krill.

Understanding how baleen whales may respond to environmental variability is increasingly important in this rapidly changing Antarctic ecosystem, where shifts in circulation, sea ice, and productivity may alter the future location and predictability of feeding habitat. By comparing acoustic occurrence data with oceanographic data, this study identifies environmental

processes that are associated with whale acoustic occurrence, revealing substantial species- and call type-specific differences, and provides a foundation for future research that aims to resolve the mechanisms underlying these relationships.

This thesis is currently being prepared for publication of the material. Schriber, Nicole; Wood, Megan; Širović, Ana; Posdaljian, Natalie; Hildebrand, John A.; Baumann-Pickering, Simone. The thesis author was the primary investigator and author of this material.

REFERENCES

Akaike, H. (1974). A new look at the statistical model identification. *IEEE Transactions on Automatic Control*, *19*(6), 716–723. https://doi.org/10.1109/TAC.1974.1100705

Alexander, P., Duncan, A., Bose, N., & Williams, G. (2016). Modelling acoustic propagation beneath Antarctic sea ice using measured environmental parameters. *Deep Sea Research Part II: Topical Studies in Oceanography, East Antarctic Sea-Ice Physics and Ecosystem Processes*, *131*, 84–95. https://doi.org/10.1016/j.dsr2.2016.04.026

Andrews-Goff, V., Bestley, S., Gales, N. J., Laverick, S. M., Paton, D., Polanowski, A. M., Schmitt, N. T., & Double, M. C. (2018). Humpback whale migrations to Antarctic summer foraging grounds through the southwest Pacific Ocean. *Scientific Reports*, *8*(1), 12333. https://doi.org/10.1038/s41598-018-30748-4

AVISO+. (2018). *Backward-in-time finite-size Lyapunov exponents (FSLEs) and orientations of the associated eigenvectors: DUACS2018 delayed-time global all-satellite product* [Data set]. SSALTO/DUACS. https://doi.org/10.24400/527896/a01-2022.002

Bloom, S., Alksne, M., Rice, A., Lankhorst, M., Širović, A., Warren, J., & Baumann-Pickering, S. (2025). Seasonal changes in physical oceanography modulate cetacean predator-prey dynamics in the San Diego Trough. *Marine Ecology Progress Series*, *762*, 111–133. https://doi.org/10.3354/meps14864

Branch, T. (2023). Abundance of Antarctic blue whales south of 60°S from three complete circumpolar sets of surveys. *J. Cetacean Res. Manage.*, *9*, 253–262. https://doi.org/10.47536/jcrm.v9i3.674

Burkhardt, E., Van Opzeeland, I., Cisewski, B., Mattmüller, R., Meister, M., Schall, E., Spiesecke, S., Thomisch, K., Zwicker, S., & Boebel, O. (2021). Seasonal and diel cycles of fin whale acoustic occurrence near Elephant Island, Antarctica. *Royal Society Open Science*, *8*(5), 201142. https://doi.org/10.1098/rsos.201142

Clarke, A., Fisher, A., Venables, H. J., Allen, L., & Davies, R. G. (2026). A 26-year record of seasonality and interannual variability in marine mammal sightings from northern Marguerite Bay, Antarctica. *Ecology and Evolution*, *16*(3), e73317. https://doi.org/10.1002/ece3.73317

Clarke, A., Murphy, E. J., Meredith, M. P., King, J. C., Peck, L. S., Barnes, D. K. A., & Smith, R. C. (2007). Climate change and the marine ecosystem of the western Antarctic Peninsula. *Philosophical Transactions of the Royal Society B: Biological Sciences*, *362*(1477), 149–166. https://doi.org/10.1098/rstb.2006.1958

Cotte, C., d'Ovidio, F., Chaigneau, A., Lèvy, M., Taupier-Letage, I., Mate, B., & Guinet, C. (2011). Scale-dependent interactions of Mediterranean whales with marine dynamics. *Limnology and Oceanography*, *56*(1), 219–232. https://doi.org/10.4319/lo.2011.56.1.0219

Croll, D. A., Acevedo-Gutiérrez, A., Tershy, B. R., & Urbán-Ramírez, J. (2001). The diving behavior of blue and fin whales: Is dive duration shorter than expected based on oxygen stores? *Comparative Biochemistry and Physiology Part A: Molecular & Integrative Physiology*, *129*(4), 797–809. https://doi.org/10.1016/S1095-6433(01)00348-8

Curtice, C., Johnston, D. W., Ducklow, H., Gales, N., Halpin, P. N., & Friedlaender, A. S. (2015). Modeling the spatial and temporal dynamics of foraging movements of humpback whales (*Megaptera novaeangliae*) in the Western Antarctic Peninsula. *Movement Ecology*, *3*(1), 13. https://doi.org/10.1186/s40462-015-0041-x

Curtis, K. R., Howe, B. M., & Mercer, J. A. (1999). Low-frequency ambient sound in the North Pacific: Long time series observations. *The Journal of the Acoustical Society of America*, *106*(6), 3189–3200. https://doi.org/10.1121/1.428173

d'Ovidio, F., De Monte, S., Alvain, S., Dandonneau, Y., & Lévy, M. (2010). Fluid dynamical niches of phytoplankton types. *Proceedings of the National Academy of Sciences*, *107*(43), 18366–18370. https://doi.org/10.1073/pnas.1004620107

d'Ovidio, F., Fernández, V., Hernández-García, E., & López, C. (2004). Mixing structures in the Mediterranean Sea from finite-size Lyapunov exponents. *Geophysical Research Letters*, *31*(17). https://doi.org/10.1029/2004GL020328

Daly, K. L. (2004). Overwintering growth and development of larval *Euphausia superba*: An interannual comparison under varying environmental conditions west of the Antarctic Peninsula. *Deep Sea Research Part II: Topical Studies in Oceanography, Integrated Ecosystem Studies of Western Antarctic Peninsula Continental Shelf Waters and Related Southern Ocean Regions*, *51*(17), 2139–2168. https://doi.org/10.1016/j.dsr2.2004.07.010

Dorschel, B., Hehemann, L., Viquerat, S., Warnke, F., Dreutter, S., Tenberge, Y. S., Accettella, D., An, L., Barrios, F., Bazhenova, E., Black, J., Bohoyo, F., Davey, C., De Santis, L., Dotti, C. E., Fremand, A. C., Fretwell, P. T., Gales, J. A., Gao, J., Gasperini, L., Greenbaum, J. S., Jencks, J. H., Hogan, K., Hong, J. K., Jakobsson, M., Jensen, L., Kool, J., Larin, S., Larter, R. D., Leitchenkov, G., Loubrieu, B., Mackay, K., Mayer, L., Millan, R., Morlighem, M., Navidad, F., Nitsche, F. O., Nogi, Y., Pertuisot, C., Post, A. L., Pritchard, H. D., Purser, A., Rebesco, M., Rignot, E., Roberts, J. L., Rovere, M., Ryzhov, I., Sauli, C., Schmitt, T., Silvano, A., Smith, J., Snaith, H., Tate, A. J., Tinto, K., Vandenbossche, P., Wetherall, P., Wintersteller, P., Yang, C., Zhang, T., Arndt, J. E. (2022). The International Bathymetric Chart of the Southern Ocean Version 2. *Scientific Data*, *9*(1), 275. https://doi.org/10.1038/s41597-022-01366-7

Ducklow, H. W., Baker, K., Martinson, D. G., Quetin, L. B., Ross, R. M., Smith, R. C., Stammerjohn, S. E., Vernet, M., & Fraser, W. (2007). Marine pelagic ecosystems: The West Antarctic Peninsula. *Philosophical Transactions of the Royal Society B: Biological Sciences*, *362*(1477), 67–94. https://doi.org/10.1098/rstb.2006.1955

E.U. Copernicus Marine Service Information. (2023). *Global Ocean Physics Reanalysis (GLOBAL_MULTIYEAR_PHY_001_030)* [Data set]. Marine Data Store. https://doi.org/10.48670/moi-00021

E.U. Copernicus Marine Service Information. (2024). *Global Ocean Biogeochemistry Hindcast (GLOBAL_MULTIYEAR_BGC_001_029)* [Data set]. Marine Data Store. https://doi.org/10.48670/moi-00019

Fahlbusch, J. A., Cade, D. E., Hazen, E. L., Elliott, M. L., Saenz, B. T., Goldbogen, J. A., & Jahncke, J. (2024). Submesoscale coupling of krill and whales revealed by aggregative Lagrangian coherent structures. *Proceedings of the Royal Society B: Biological Sciences*, *291*(2017), 20232461. https://doi.org/10.1098/rspb.2023.2461

Fox, J., & Weisberg, S. (2019). *An R Companion to Applied Regression* (3rd ed.). SAGE publications. https://www.john-fox.ca/Companion/

Friedlaender, A., Halpin, P., Qian, S., Lawson, G., Wiebe, P., Thiele, D., & Read, A. (2006). Whale distribution in relation to prey abundance and oceanographic processes in shelf waters of Western Antarctic Peninsula. *Marine Ecology Progress Series*, *317*, 297–310. https://doi.org/10.3354/meps317297

García, M. A., Castro, C. G., Ríos, A. F., Doval, M. D., Rosón, G., Gomis, D., & López, O. (2002). Water masses and distribution of physico-chemical properties in the Western Bransfield Strait and Gerlache Strait during Austral summer 1995/96. *Deep Sea Research Part II: Topical Studies in Oceanography, FRUELA - A Carbon Flux Study in the Antarctic Peninsula Area*, *49*(4), 585–602. https://doi.org/10.1016/S0967-0645(01)00113-8

Haberman, K. L., Ross, R. M., & Quetin, L. B. (2003). Diet of the Antarctic krill (*Euphausia superba* Dana): II. Selective grazing in mixed phytoplankton assemblages. *Journal of Experimental Marine Biology and Ecology*, *283*(1), 97–113. https://doi.org/10.1016/S0022-0981(02)00467-7

Harrison, L.-M. K., Goetz, K., Cox, M. J., & Harcourt, R. (2020). A Southern Ocean archipelago enhances feeding opportunities for a krill predator. *Marine Mammal Science*, *36*(1), 260–275. https://doi.org/10.1111/mms.12645

Hastie, T. J., & Tibshirani, R. J. (1990). *Generalized Additive Models*. CRC Press.

Helble, T. A., Ierley, G. R., D'Spain, G. L., Roch, M. A., & Hildebrand, J. A. (2012). A generalized power-law detection algorithm for humpback whale vocalizations. *The Journal of the Acoustical Society of America*, *131*(4), 2682–2699. https://doi.org/10.1121/1.3685790

Herr, H., Viquerat, S., Devas, F., Lees, A., Wells, L., Gregory, B., Giffords, T., Beecham, D., & Meyer, B. (2022). Return of large fin whale feeding aggregations to historical whaling grounds in the Southern Ocean. *Scientific Reports*, *12*(1), 9458. https://doi.org/10.1038/s41598-022-13798-7

Herr, H., Viquerat, S., Siegel, V., Kock, K.-H., Dorschel, B., Huneke, W. G. C., Bracher, A., Schröder, M., & Gutt, J. (2016). Horizontal niche partitioning of humpback and fin whales around the West Antarctic Peninsula: Evidence from a concurrent whale and krill survey. *Polar Biology*, *39*(5), 799–818. https://doi.org/10.1007/s00300-016-1927-9

Jiang, M., Charette, M. A., Measures, C. I., Zhu, Y., & Zhou, M. (2013). Seasonal cycle of circulation in the Antarctic Peninsula and the off-shelf transport of shelf waters into southern Drake Passage and Scotia Sea. *Deep Sea Research Part II: Topical Studies in Oceanography, Southern Ocean Natural Iron Fertilization*, *90*, 15–30. https://doi.org/10.1016/j.dsr2.2013.02.029

Johannessen, J. E. D., Biuw, M., Lindstrøm, U., Ollus, V. M. S., Martín López, L. M., Gkikopoulou, K. C., Oosthuizen, W. C., & Lowther, A. (2022). Intra-season variations in distribution and abundance of humpback whales in the West Antarctic Peninsula using cruise vessels as opportunistic platforms. *Ecology and Evolution*, *12*(2), e8571. https://doi.org/10.1002/ece3.8571

Jones, J. M., Hildebrand, J. A., Thayre, B. J., Jameson, E., Small, R. J., & Wiggins, S. M. (2022). The influence of sea ice on the detection of bowhead whale calls. *Scientific Reports*, *12*(1), 8553. https://doi.org/10.1038/s41598-022-12186-5

Krumhardt, K. M., Long, M. C., Sylvester, Z. T., & Petrik, C. M. (2022). Climate drivers of Southern Ocean phytoplankton community composition and potential impacts on higher trophic levels. *Frontiers in Marine Science*, *9*. https://doi.org/10.3389/fmars.2022.916140

Lavery, T. J., Roudnew, B., Seymour, J., Mitchell, J. G., Smetacek, V., & Nicol, S. (2014). Whales sustain fisheries: Blue whales stimulate primary production in the Southern Ocean. *Marine Mammal Science*, *30*(3), 888–904. https://doi.org/10.1111/mms.12108

Laws, R. M. (1977). Seals and whales of the Southern Ocean. *Philosophical Transactions of the Royal Society of London. B, Biological Sciences*, *279*(963), 81–96. https://doi.org/10.1098/rstb.1977.0073

Loeb, V., Hofmann, E., Klinck, J., & Holm-Hansen, O. (2010). Hydrographic control of the marine ecosystem in the South Shetland-Elephant Island and Bransfield Strait region. *Deep Sea Research Part II: Topical Studies in Oceanography*, *57*, 519–542. https://doi.org/10.1016/j.dsr2.2009.10.004

Marques, T. A., Thomas, L., Martin, S. W., Mellinger, D. K., Ward, J. A., Moretti, D. J., Harris, D., & Tyack, P. L. (2013). Estimating animal population density using passive acoustics. *Biological Reviews*, *88*(2), 287–309. https://doi.org/10.1111/brv.12001

McDonald, M. A., Mesnick, S. L., & Hildebrand, J. A. (2006). Biogeographic characterization of blue whale song worldwide: Using song to identify populations. *Journal of Cetacean Research and Management*, *8*(1), 55–65.

Mellinger, D., Stafford, K., Moore, S., Dziak, B., & Matsumoto, H. (2007). An overview of fixed passive acoustic observation methods for cetaceans. *Oceanography*, *20*, 36–45. https://doi.org/10.5670/oceanog.2007.03

Menze, S., Zitterbart, D. P., Van Opzeeland, I., & Boebel, O. (2017). The influence of sea ice, wind speed and marine mammals on Southern Ocean ambient sound. *Royal Society Open Science*, *4*(1), 160370. https://doi.org/10.1098/rsos.160370

Miller, B. S., Andrews-Goff, V., Barlow, J., Bell, E., Calderan, S., Double, M. C., Gedamke, J., Kelly, N., Laverick, S., Leaper, R., Miller, E. J., Reeve, K., Širović, A., & Stafford, K. M. (2024). Antarctic sonobuoy surveys for blue whales from 2006-2021 reveal contemporary distribution, changes over time, and paths to further our understanding of their distribution and biology. *Frontiers in Marine Science*, *11*. https://doi.org/10.3389/fmars.2024.1324816

Miller, E. J., Potts, J. M., Cox, M. J., Miller, B. S., Calderan, S., Leaper, R., Olson, P. A., O'Driscoll, R. L., & Double, M. C. (2019). The characteristics of krill swarms in relation to aggregating Antarctic blue whales. *Scientific Reports*, *9*(1), 16487. https://doi.org/10.1038/s41598-019-52792-4

Murase, H., Matsuoka, K., Ichii, T., & Nishiwaki, S. (2002). Relationship between the distribution of euphausiids and baleen whales in the Antarctic (35°E – 145°W). *Polar Biology*, *25*(2), 135–145. https://doi.org/10.1007/s003000100321

Nicol, S. (2006). Krill, Currents, and Sea Ice: *Euphausia superba* and its changing environment. *BioScience*, *56*(2), 111–120. https://doi.org/10.1641/0006-3568(2006)056[0111:KCASIE]2.0.CO;2

Nicol, S., Bowie, A., Jarman, S., Lannuzel, D., Meiners, Klaus M., & van der Merwe, P. (2010). Southern Ocean iron fertilization by baleen whales and Antarctic krill. *Fish and Fisheries*, *11*(2), 203–209. https://doi.org/10.1111/j.1467-2979.2010.00356.x

Nicol, S., Worby, A., & Leaper, R. (2008). Changes in the Antarctic sea ice ecosystem: Potential effects on krill and baleen whales. *Marine & Freshwater Research*, *59*(5), 361–382. https://doi.org/10.1071/MF07161

Nieukirk, S. L., Mellinger, D. K., Moore, S. E., Klinck, K., Dziak, R. P., & Goslin, J. (2012). Sounds from airguns and fin whales recorded in the mid-Atlantic Ocean, 1999-2009. *The Journal of the Acoustical Society of America*, *131*(2), 1102–1112. https://doi.org/10.1121/1.3672648

Nowacek, D. P., Friedlaender, A. S., Halpin, P. N., Hazen, E. L., Johnston, D. W., Read, A. J., Espinasse, B., Zhou, M., & Zhu, Y. (2011). Super-aggregations of krill and humpback whales in Wilhelmina Bay, Antarctic Peninsula. *PLOS ONE*, *6*(4), e19173. https://doi.org/10.1371/journal.pone.0019173

Oleson, E. M., Calambokidis, J., Burgess, W. C., McDonald, M. A., LeDuc, C. A., & Hildebrand, J. A. (2007). Behavioral context of call production by eastern North Pacific blue whales. *Marine Ecology Progress Series*, *330*, 269–284. https://doi.org/10.3354/meps330269

Panigada, S., Panigada, V., Hickmott, L., Kennedy, A., & Herr, H. (2024). Insights into fin whale movements and foraging behaviour around Elephant Island, Antarctica. [Special issue 5] *J. Cetacean Res. Manage.*, 167–178. https://doi.org/10.47536/jcrm.v5i1.1099

Patterson, S. L., & Sievers, H. A. (1980). The Weddell-Scotia Confluence. *Journal of Physical Oceanography*, *10*(10), 1584–1610. https://doi.org/10.1175/1520-0485(1980)010%3C1584:TWSC%3E2.0.CO;2

Price, H. J., Boyd, K. R., & Boyd, C. M. (1988). Omnivorous feeding behavior of the Antarctic krill *Euphausia superba*. *Marine Biology*, *97*(1), 67–77. https://doi.org/10.1007/BF00391246

R Core Team. (2025). *R: A language and environment for statistical computing* [Computer software]. R Foundation for Statistical Computing. https://www.R-project.org/

Rocha, J., Clapham, P., & Ivashchenko, Y. (2015). Emptying the oceans: A summary of industrial whaling catches in the 20th century. *Marine Fisheries Review*, *76*, 37–48. https://doi.org/10.7755/MFR.76.4.3

Roman, J., Abraham, A. J., Kiszka, J. J., Costa, D. P., Doughty, C. E., Friedlaender, A., Hückstädt, L. A., Marcondes, M., Wetsel, E., & Pershing, A. J. (2025). Migrating baleen whales transport high-latitude nutrients to tropical and subtropical ecosystems. *Nature Communications*, *16*(1), 2125. https://doi.org/10.1038/s41467-025-56123-2

Saba, G. K., Fraser, W. R., Saba, V. S., Iannuzzi, R. A., Coleman, K. E., Doney, S. C., Ducklow, H. W., Martinson, D. G., Miles, T. N., Patterson-Fraser, D. L., Stammerjohn, S. E., Steinberg, D. K., & Schofield, O. M. (2014). Winter and spring controls on the summer food web of the coastal West Antarctic Peninsula. *Nature Communications*, *5*(1), 4318. https://doi.org/10.1038/ncomms5318

Sangrà, P., Gordo, C., Hernández-Arencibia, M., Marrero-Díaz, A., Rodríguez-Santana, A., Stegner, A., Martínez-Marrero, A., Pelegrí, J. L., & Pichon, T. (2011). The Bransfield current system. *Deep Sea Research Part I: Oceanographic Research Papers*, *58*(4), 390–402. https://doi.org/10.1016/j.dsr.2011.01.011

Santora, J., Reiss, C., Loeb, V., & Veit, R. (2010). Spatial association between hotspots of baleen whales and demographic patterns of Antarctic krill *Euphausia superba* suggests size-dependent predation. *Marine Ecology Progress Series*, *405*, 255–269. https://doi.org/10.3354/meps08513

Schall, E., Thomisch, K., Boebel, O., Gerlach, G., Spiesecke, S., & Van Opzeeland, I. (2020). Large-scale spatial variabilities in the humpback whale acoustic presence in the Atlantic sector of the Southern Ocean. *Royal Society Open Science*, *7*(12), 201347. https://doi.org/10.1098/rsos.201347

Seyboth, E., Meynecke, J.-O., de Bie, J., Roychoudhury, A., & Findlay, K. (2023). A review of post-whaling abundance, trends, changes in distribution and migration patterns, and supplementary feeding of Southern Hemisphere humpback whales. *Frontiers in Marine Science*, *10*, https://doi.org/10.3389/fmars.2023.997491

Shabangu, F., Andrew, R., Yemane, D., & Findlay, K. (2020). Acoustic seasonality, behaviour and detection ranges of Antarctic blue and fin whales under different sea ice conditions off Antarctica. *Endangered Species Research*, *43*, 21–37. https://doi.org/10.3354/esr01050

Silk, J. R. D., Thorpe, S. E., Fielding, S., Murphy, E. J., Trathan, P. N., Watkins, J. L., & Hill, S. L. (2016). Environmental correlates of Antarctic krill distribution in the Scotia Sea and southern Drake Passage. *ICES Journal of Marine Science*, *73*(9), 2288–2301. https://doi.org/10.1093/icesjms/fsw097

Simpson, G. L. (2024). gratia: An R package for exploring generalized additive models. *Journal of Open Source Software*, *9*(104), 6962. https://doi.org/10.21105/joss.06962

Širović, A., & Hildebrand, J. A. (2011). Using passive acoustics to model blue whale habitat off the Western Antarctic Peninsula. *Deep Sea Research Part II: Topical Studies in Oceanography, Understanding the Linkages between Antarctic Food Webs and the Environment: A Synthesis of Southern Ocean GLOBEC Studies*, *58*(13), 1719–1728. https://doi.org/10.1016/j.dsr2.2010.08.019

Širović, A., Hildebrand, J. A., & Wiggins, S. M. (2007). Blue and fin whale call source levels and propagation range in the Southern Ocean. *The Journal of the Acoustical Society of America*, *122*(2), 1208–1215. https://doi.org/10.1121/1.2749452

Širović, A., Hildebrand, J. A., Wiggins, S. M., McDonald, M. A., Moore, S. E., & Thiele, D. (2004). Seasonality of blue and fin whale calls and the influence of sea ice in the Western Antarctic Peninsula. *Deep Sea Research Part II: Topical Studies in Oceanography*, *51*(17–19), 2327–2344. https://doi.org/10.1016/j.dsr2.2004.08.005

Širović, A., Hildebrand, J. A., Wiggins, S. M., & Thiele, D. (2009). Blue and fin whale acoustic presence around Antarctica during 2003 and 2004. *Marine Mammal Science*, *25*(1), 125–136. https://doi.org/10.1111/j.1748-7692.2008.00239.x

Smith, M. E. K., Ososky, J. J., Hunt, K. E., Cioffi, W. R., Read, A. J., Friedlaender, A. S., McCarthy, M., & Fleming, A. H. (2024). Historical baleen plates indicate that once abundant Antarctic blue and fin whales demonstrated distinct migratory and foraging strategies. *Ecology and Evolution*, *14*(5), e11376. https://doi.org/10.1002/ece3.11376

Tang, Y., Horikoshi, M., & Li, W. (2016). The R Journal: Ggfortify: Unified interface to visualize statistical results of popular R packages. *The R Journal*, *8*(2), 474–485. https://doi.org/10.32614/RJ-2016-060

Thiele, D., Chester, E. T., Moore, S. E., Širovic, A., Hildebrand, J. A., & Friedlaender, A. S. (2004). Seasonal variability in whale encounters in the Western Antarctic Peninsula. *Deep Sea Research Part II: Topical Studies in Oceanography, Integrated Ecosystem Studies of Western Antarctic Peninsula Continental Shelf Waters and Related Southern Ocean Regions*, *51*(17), 2311–2325. https://doi.org/10.1016/j.dsr2.2004.07.007

Thomisch, K., Boebel, O., Clark, C. W., Hagen, W., Spiesecke, S., Zitterbart, D. P., & Van Opzeeland, I. (2016). Spatio-temporal patterns in acoustic presence and distribution of Antarctic blue whales *Balaenoptera musculus intermedia* in the Weddell Sea. *Endangered Species Research*, *30*, 239–253. https://doi.org/10.3354/esr00739

Thompson, A. F., Heywood, K. J., Thorpe, S. E., Renner, A. H. H., & Trasviña, A. (2009). Surface circulation at the tip of the Antarctic Peninsula from drifters. *Journal of Physical Oceanography*, *39*(1), 3–26. https://doi.org/10.1175/2008JPO3995.1

Tokarczyk, R. (1987). Classification of water masses in the Bransfield Strait and southern part of the Drake Passage using a method of statistical multidimensional analysis. *Polish Polar Research*, *8*(4), 333–366.

Trathan, P. N., Savoca, M. S., Friedlaender, A., Baines, M., Burkhardt, E., Cheeseman, T., Dalla Rosa, L., Herr, H., Secchi, E. R., Zerbini, A. N., & Reisinger, R. R. (2024). Integrating the needs of recovering populations of baleen whales into the revised management framework for the commercial fishery for Antarctic krill. *Frontiers in Marine Science*, *11*. https://doi.org/10.3389/fmars.2024.1458042

Van Opzeeland, I., Van Parijs, S., Kindermann, L., Burkhardt, E., & Boebel, O. (2013). Calling in the cold: Pervasive acoustic presence of humpback whales (*Megaptera novaeangliae*) in Antarctic Coastal Waters. *PLOS ONE*, *8*(9), e73007. https://doi.org/10.1371/journal.pone.0073007

Ware, C., Friedlaender, A. S., & Nowacek, D. P. (2011). Shallow and deep lunge feeding of humpback whales in fjords of the West Antarctic Peninsula. *Marine Mammal Science*, *27*(3), 587–605. https://doi.org/10.1111/j.1748-7692.2010.00427.x

Watkins, W. A., Daher, M. A., Reppucci, G. M., George, J. E., Martin, D. L., DiMarzio, N. A., & Gannon, D. P. (2000). Seasonality and distribution of whale calls in the North Pacific. *Oceanography*, *13*(1), 62–67.

Welch, P. (1967). The use of fast Fourier transform for the estimation of power spectra: A method based on time averaging over short, modified periodograms. *IEEE Transactions on Audio and Electroacoustics*, *15*(2), 70–73. https://doi.org/10.1109/TAU.1967.1161901

Whitehouse, M. J., Atkinson, A., Ward, P., Korb, R. E., Rothery, P., & Fielding, S. (2009). Role of krill versus bottom-up factors in controlling phytoplankton biomass in the northern Antarctic waters of South Georgia. *Marine Ecology Progress Series*, *393*, 69–82. https://doi.org/10.3354/meps08288

Wiggins, S. M., & Hildebrand, J. A. (2007). High-frequency Acoustic Recording Package (HARP) for broad-band, long-term marine mammal monitoring. *International Symposium on Underwater Technology 2007 and International Workshop on Scientific Use of Submarine Cables & Related Technologies 2007*, *UT07*, 551–557.

Wiggins, S. M., Roch, M. A., & Hildebrand, J. A. (2010). TRITON software package: Analyzing large passive acoustic monitoring data sets using MATLAB. *The Journal of the Acoustical Society of America*, *128*(4_Supplement), 2299–2299. https://doi.org/10.1121/1.3508074

Wood, S. N. (2011). Fast stable restricted maximum likelihood and marginal likelihood estimation of semiparametric generalized linear models. *Journal of the Royal Statistical Society Series B: Statistical Methodology*, *73*(1), 3–36. https://doi.org/10.1111/j.1467-9868.2010.00749.x

Wood, S. N. (2013). On p-values for smooth components of an extended generalized additive model. *Biometrika*, *100*(1), 221–228. https://doi.org/10.1093/biomet/ass048